

SUBMISSION TO
S-.T.YAU HIGH SCHOOL SCIENCE AWARD (PHYSICS)

The Winding Pendulum Phenomenon

A study on pendula with azimuthal-length constraint

Schools:

Harbin Normal University High School
Dalian Yuming High School

Province & Country/Region:

Heilongjiang, China

Members:

Zhaoyi LI
Sifei ZHANG

Supervisors:

Shiqiang DENG
Yongyuan JIANG



Tlalauhqui Tezcatlipoca [t̪laːt̪awːkiː teskat̪liːpoːka]
(God related to the pole dance)

Statement of Originality

This team declares that the submitted paper is the result of the research done in the supervision of the advisor. To this team's knowledge, apart from the contents that are in-text cited or listed in acknowledgement, this paper does not include any research from others' work or from anything this team has written or has published. If our statement is anyway untrue, we bear all legal responsibilities.

Team members' Signatures:



Supervisors' Signatures:



September 14, 2018

Abstract

Inspired by the **Danza de los Voladores** (Dance of the Flyers), a traditional Mexican performance, we investigated an interesting dynamical phenomenon and conducted this research. To the best of our knowledge, no relevant research related to this phenomenon have been done up till now and the reasons behind the trajectory of the performers are still unknown. In this study, a simple theoretical model is set up firstly to qualitatively explain the phenomenon and a more realistic model is used to give out more clear explanations. Secondly, numerical simulations are done and the results are discussed in details. Finally, experiments are carried out to verify the results of simulations. Throughout the research, scientific calculating languages such as MATLAB and Mathematica are used to generate the figure, extract the data and analyze the video. The final experimental results are in accordance with the simulation. The basic characteristics, including the oscillation of the latitudinal angular motion, the asymptotic motion, and the monotonic characteristics of the azimuthal angle of the phenomenon are explained. In addition, the experimental data give rise to short discussions about some interesting phenomena.

Besides directly explaining the questions we proposed and accurately describing the characteristics of the motion, the results of this research have extra potential benefits. Due to the abundance of pendula-related physics phenomena, this study can offer explanation, guidance and directions for all kinds of future studies. Furthermore, real world mechanical applications related to the crane pulleys, twisted earphones and high-voltage wires can be understood more clearly based on the results of this research. Some inspirations on theoretical physics can also be drawn from this research. Last but not least, this research offers a simple but interesting model for physics discussions and education. It can offer people a chance to comprehend analytical mechanics more clearly.

Keywords: Pendulum, Unwinding motion, Azimuthal angle constraint, Experimentation, Kinematics characteristics

Contents

Abstract	iii
Table of contents	iv
1 Introduction	1
1.1 Some Inspiration	1
1.2 Background Information	1
1.3 Significance of the study	3
1.4 Nomenclatures	4
1.5 List of Variables and Constants	5
2 Theoretical Model	6
2.1 Overview	6
2.2 Simplified Model	7
2.2.1 The setup of the model	7
2.2.2 A Seemingly Paradoxical Problem	14
2.3 Solution to the Original Problem	15
2.4 A Model involving the involute	15
2.4.1 The setup of the model	15
2.4.2 Final results of the simulation	19
2.4.3 Discussion of the possible values of ϕ	22
2.5 Model of the original problem	24
3 Experiments	25
3.1 Overview	25
3.2 Experiment setup	25
3.2.1 Trial 1&2	26
3.2.2 Trial 3-7	29
3.2.3 About the sliding problem	32
3.3 Data Analysis	36
3.3.1 Collection of the data	36
3.3.2 Error Analysis	39
4 Conclusions	42
5 Prospect	42
Reference	43
Acknowledgements	44
Appendix	45
A List of Graphics	45
B List of Tables	46
C Mathematica Codes	48
D Matlab Code	57

1 Introduction

1.1 Some Inspiration

All this began when the team leader Zhaoyi Li was at a physics camp during the spring of 2018, a question about the conical pendulum in an experiment class attracts his attention. The original problem goes as follows:

“ Suppose the length of the pendulum is changing over time, and the period T satisfies a linear relationship with the number of unwinding, n , find the experimental formula $T \propto n^\alpha$.”

Knowing the teacher’s intention is to do the experiment and get the relationship experimentally, Zhaoyi Li is fascinated by the theory behind this motion. The conical pendulum motion is simple and easy to comprehend, but what if the pendulum unwinds over time? The motion will be much more complex, and this phenomenon is surely interesting to research on. After looking up for all kinds of materials online, Zhaoyi Li found out that no preceding research related to this particular motion were done and this research may bring up some fascinating discoveries.

Surprisingly, when Zhaoyi Li was at Stanford Summer College, he accidentally met a physics instructor who is from Mexico and learned that there is a traditional Mexican performance, the **Danza de los Voladores**, which contains similar physical phenomenon to create magnificent art effects. This real-world application makes this research more utilitarian and fun to conduct. It was not before long when Sifei Zhang showed her interest to the phenomenon and joined the research, the group of two is finally founded and the study is conducted.

1.2 Background Information

The **Danza de los Voladores** (Dance of the Flyers) , a traditional Mexican ritual, is a plea for gods to end droughts. It starts with climbing of a tall pole and dancing. Then, four performers jump off from the top of the pole with ropes tied on their feet. During this process, they rotate around the pole as the rope is unwound from the pole[1], as shown in Fig.1. Their velocities, as well as their relative positions to each other display a change during the performance and they land on the ground with relatively small velocity at the end of the performance.



Figure 1 Danza de los Voladores (Dance of the Flyers)[2]

The motion of the dancers can be treated as a conical pendulum whose string length depends on the turns it unwinds. As the system evolves through time, gravitational potential continuously transforms into kinetic energy but the moment of inertia of the whole system also increases, thus the angular velocity displays a oscillatory change, and the trajectories of each single point of mass (performers) are unique.

The unwinding mechanism is carried out by the simple device on the top of the pole, as shown in Fig.2.



Figure 2 Details of the pole

As the ropes are wound on the pole, the constraining relationship exists that the rope length is directly proportional to the azimuthal angle.

1.3 Significance of the study

1. The winding pendulum phenomenon occurs frequently in daily life, such as crane pulleys and pendula that are twisted and not well functioning. The research can offer inspiration, explanation and researching direction for these phenomena.
2. Pendula problems are an important portion of mechanics, the research can fill a “missed piece” of the category of all pendula, giving experimental data and explanations to pendula problems.
3. The research can offer explanation to the patterns and visual effects generated by the performers in **Danza de los Voladores**, identifying security risks related to the performance due to the sudden-sliding phenomenon.
4. The problem can offer insights to theoretical mechanics discussions, such as whether a Lagrangian is “correct” when the motion cannot occur in real world.
5. The problem itself is an interesting physics model that is worth discussing. It can offer more inspiration on physics classes or discussions and be beneficial to future physics education.

1.4 Nomenclatures

For the convenience of discussion, different parts of the winding pendulum are referred to as shown in Fig.3.

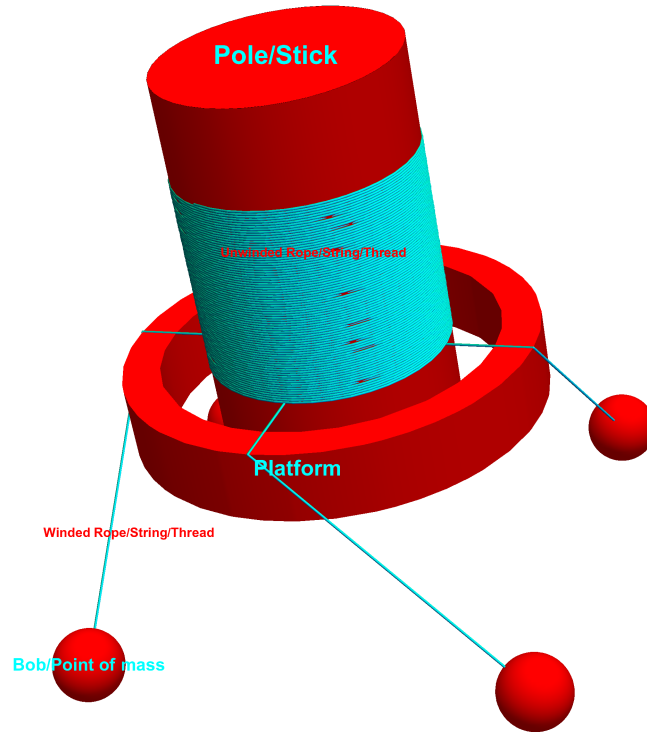


Figure 3 The winding pendulum model

The pole, or stick, is the middle part on which the string, wire, or rope is wound, a bob, or point of mass is attached to the end of the string and moves. The platform is the sustaining part on the top of the pole, over which the rope is crossed and suspended. During the motion, it functions as not only a pulley to change the direction of the tension on the rope, but also synchronize the motion of the four pendula. Its another function is to avoid sudden sliding of the rope, which is explained in more details in Part 3.2.3.

1.5 List of Variables and Constants

Table 1 shows the name of variables included in this paper.

Table 1 List of Variables

Variable name	Quantity	Unit
t	Time	s
T	Period	s
m	Mass of the bob	kg
σ	Line mass of the rope	kg m ⁻¹
g	Gravity constant	kg s ⁻²
T	Tension	N
λ	Lagrangian Multiplier	N
f	Friction	N
N	Normal force	N
l	Length of the string	m
R	Radius of the pole	m
r	Radius of the platform	m
\mathcal{L}	System Lagrangian	J
\mathcal{H}	System Hamiltonian	J
E	Total energy	J
K	Total kinetic energy	J
V	Total potential energy	J
U_{eff}	Effective potential	J
θ	Azimuthal angle	1
$\dot{\theta} = \omega$	Azimuthal angular velocity	s ⁻¹
$\ddot{\theta}$	Azimuthal angular acceleration	s ⁻²
ϕ	Latitudinal angle	1
$\dot{\phi}$	Latitudinal angular velocity	s ⁻¹
$\ddot{\phi}$	Latitudinal angular acceleration	s ⁻²
a	Shorter radius of ellipse	m
b	Longer radius of ellipse	m
ρ	Radius of curvature	m

Variable Name	Quantity	Unit
α	Auxiliary angle, arbitrary constant	1
β, n	Arbitrary constant	1
μ	Fraction coefficient of the pole	1
Δ	Relative error	1
\mathbf{r}	Auxiliary length	m
A, B, C, D, E, K, L	Arbitrary constant	1
$\mathbf{C}, \mathbf{C}_1, \mathbf{C}_2$	Constant in solutions	1

2 Theoretical Model

2.1 Overview

To simplify the problem[3], the first model is set up considering the case with only one bob while excluding the effect of the thickness of the pole, the thickness of the rope and the air resistance, i.e. consider the pole to be infinitely thin. Thus, the whole system reduces to a system with only 2D.O.Fs ϕ and θ . This model can offer a simple way to qualitatively explain the phenomenon.

The second and realistic model takes the radius of the pole into account and the rope will unwind as the bob moves in a certain trajectory. Implementing this condition into the model makes it more realistic and numerical calculations are done to explain the phenomenon.

Finally, the question 1 mentioned at the beginning of the paper is briefly discussed, and the modeling of the phenomenon in the **Danza de los Voladores** is done.

2.2 Simplified Model

2.2.1 The setup of the model

The diagram of the simplified model is shown in Fig.4.

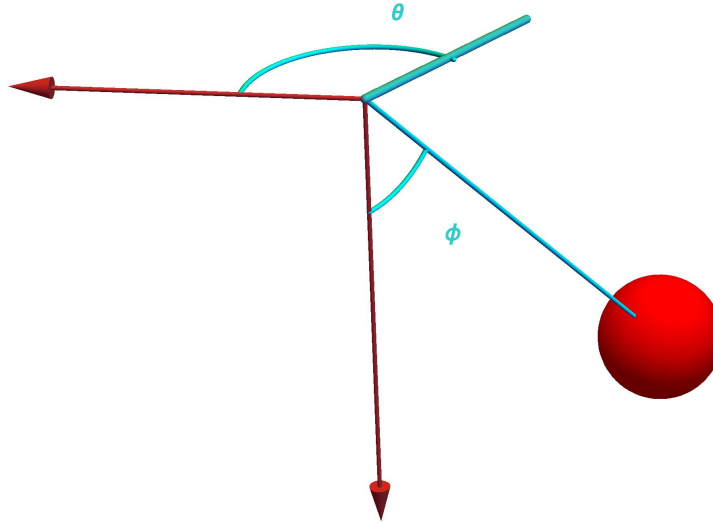


Figure 4 The two degrees of freedoms in the model

By the constraint condition:

$$l \equiv R\theta \quad (2.1)$$

We can take the derivative on both side and get

$$\dot{l} \equiv R\dot{\theta} \quad (2.2)$$

$$\ddot{l} \equiv R\ddot{\theta} \quad (2.3)$$

The Lagrangian of the system is:

$$\mathcal{L} = \frac{mR^2}{2}\dot{\theta}^2 + \frac{mR^2}{2}\dot{\theta}^2\theta^2 \sin^2 \phi + \frac{mR^2}{2}\dot{\phi}^2\theta^2 + mgR\theta \cos \phi \quad (2.4)$$

Since the Lagrangian satisfies $\frac{\partial L}{\partial t} = 0$, the system is conservative. Then, we can solve the E-L equations of the motion numerically:

$$\begin{cases} \frac{d}{dt} \frac{\partial \mathcal{L}}{\partial \dot{\theta}} = \frac{\partial \mathcal{L}}{\partial \theta} \\ \frac{d}{dt} \frac{\partial \mathcal{L}}{\partial \dot{\phi}} = \frac{\partial \mathcal{L}}{\partial \phi} \end{cases} \quad (2.5)$$

By using the following initial conditions in Table 2, quantitative answer will be given.

Table 2 Initial conditions of the simulation

Variables	g	R	m	θ_0	$\dot{\theta}_0$	ϕ_0	$\dot{\phi}_0$
Initial values	1	1	1	0.001	0	$\frac{\pi}{8}$	0

From Fig.5 and Fig.6, we can see that the latitudinal angle is oscillatory decreasing, and the longitudinal angle is relatively unstable at the beginning of the motion, but tends to a certain limit since the conservation of angular momentum ensures the bob to have a gradually decreasing speed.

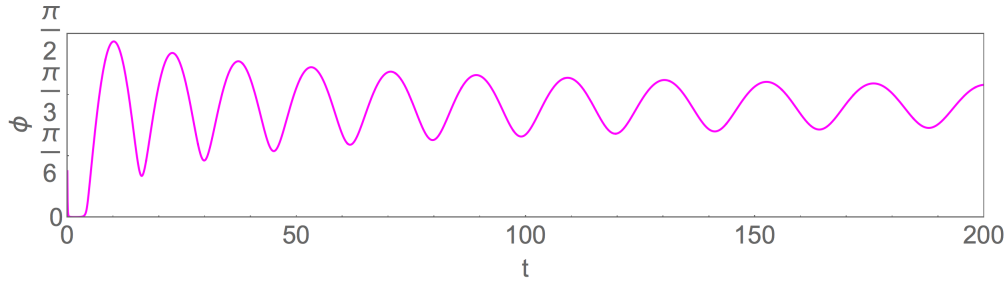


Figure 5 ϕ v.s. t plot of the result

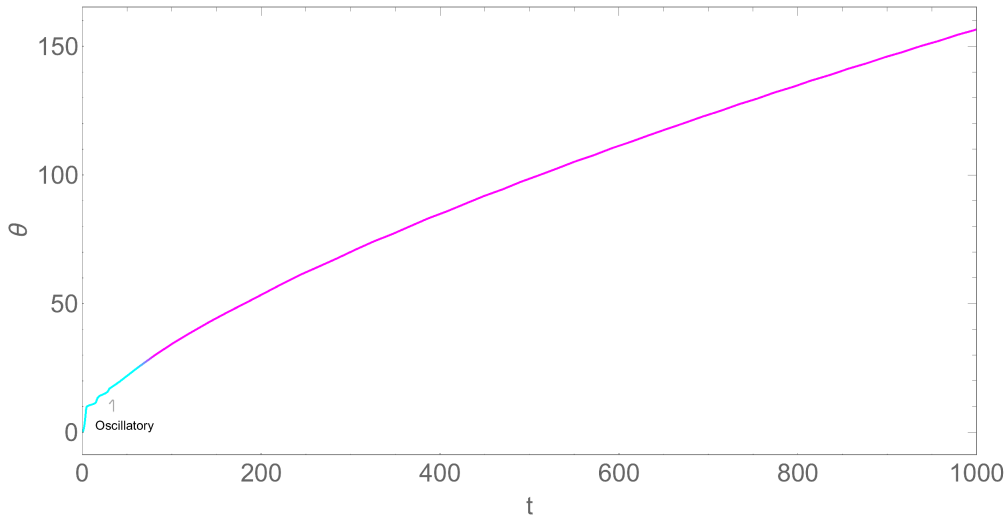


Figure 6 θ v.s. t plot of the result

This can be seen from a log-log plot of the ϕ v.s. t relation, as shown in Fig.7.

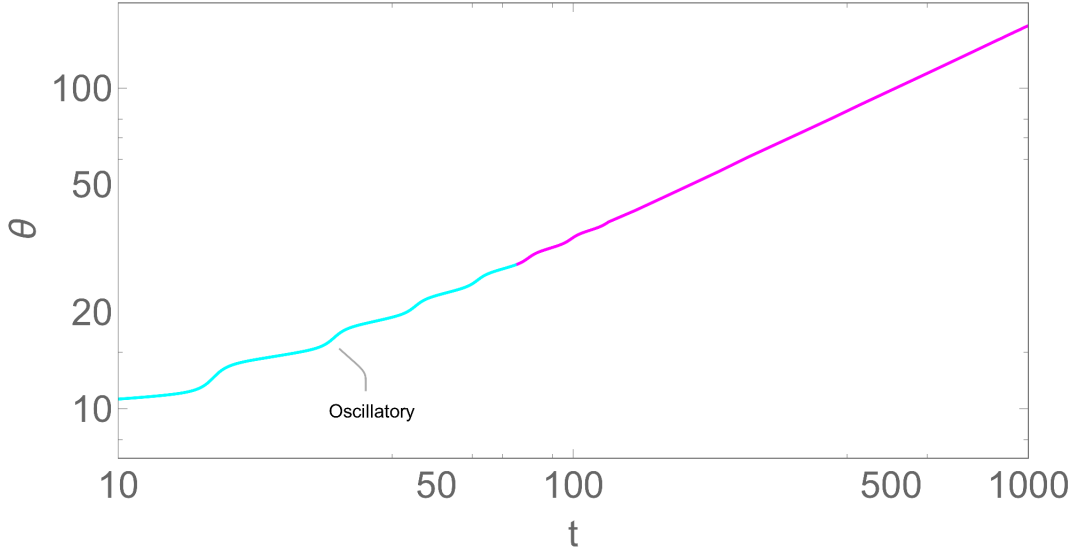


Figure 7 log-log plot of the result

The above result is convincing because when the time is enough large ($t \gg 0$), the radius of the pole is relatively small compared with the length of the thread. i.e. $R \ll l$. Thus, we can start from suitable approximation of the equations of motions, which is, explicitly:

$$\begin{cases} g \cos \phi = R\ddot{\theta} + R\theta^2\ddot{\theta} \sin^2 \phi + R\theta^2\dot{\theta}\dot{\phi} \sin 2\phi \\ g \sin \phi = -\ddot{\phi}R\theta - 2\phi R\dot{\theta} \end{cases} \quad (2.6)$$

Since $R \ll l = R\theta$, $\theta \gg 0$, we can drop the term $R\ddot{\theta}$ since it is the only term doesn't contain θ on the RHS of. Thus, we can get:

$$\begin{cases} \frac{g}{R} \cos \phi = \theta^2 \left(\ddot{\theta} \sin^2 \phi + \theta^2 \dot{\phi}\dot{\theta} \sin 2\phi \right) \\ \frac{g}{R} \sin \phi = -\ddot{\phi}\theta - 2\phi\dot{\theta} \end{cases} \quad (2.7)$$

Next, we can average the motion within a period of revolution:

$$\overline{f(t)} = \frac{\oint f(t) dt}{\oint dt} \quad (2.8)$$

Thus, from the linearity of the averaging operation, we can get:

$$\begin{cases} \frac{g}{R} \overline{\cos \phi} = \overline{\theta^2 \ddot{\theta} \sin^2 \phi} + \overline{\theta^2 \dot{\phi}\dot{\theta} \sin 2\phi} \\ \frac{g}{R} \overline{\sin \phi} = -\overline{\ddot{\phi}\theta} - 2\overline{\phi\dot{\theta}} \end{cases} \quad (2.9)$$

On the other hand, since ϕ is oscillatory approaching a certain value, the average value of $\phi(t)$ will be a constant, denoted by $\bar{\phi}$. The average value of functions containing only ϕ , such as $\sin \phi(t)$ and $\cos \phi(t)$ will be $\sin \bar{\phi}$ and $\cos \bar{\phi}$, etc. Thus, we can get the following relationship:

$$\begin{cases} \frac{g}{R} \cos \bar{\phi} = \theta^2 \left(\overline{\ddot{\theta} \sin^2 \phi} + \overline{\dot{\phi} \dot{\theta} \sin 2\phi} \right) \\ \frac{g}{R} \sin \bar{\phi} = -\overline{\dot{\phi} \theta} - 2\overline{\phi \dot{\theta}} \end{cases} \quad (2.10)$$

Since the LHS of equation is a constant, it is apparent that the quantities on the RHS, $\overline{\ddot{\theta} \sin^2 \phi}$ and $\overline{\dot{\phi} \dot{\theta} \sin 2\phi}$, should be approximately on the same order. Thus we can write it as

$$\overline{\dot{\phi} \dot{\theta} \sin 2\phi} = \mathbb{D} \overline{\ddot{\theta} \sin^2 \phi} \quad (2.11)$$

$$\frac{g}{R} \cos \bar{\phi} = \theta^2 \overline{\ddot{\theta} \sin^2 \phi} (1 + \mathbb{D}) \quad (2.12)$$

where \mathbb{D} is some arbitrary constant. Due to the fact that $\ddot{\theta}(t)$ is extremely small and $\sin \phi$ is a number with a small oscillation term when t is big enough, if we model these quantities as

$$\begin{cases} \ddot{\theta} = \epsilon_1 \sin(t) \\ \sin^2(\phi) = \epsilon_2 \sin(t) + A \end{cases} \quad (2.13)$$

The following relationships hold:

$$\begin{aligned} & \overline{\epsilon_1 \sin(t) (A + \epsilon_2 \sin(t))} \\ &= \overline{\epsilon_1 A \sin(t) + \epsilon_1 \epsilon_2 \sin^2(t)} \\ &= \overline{\epsilon A \sin(t)} \\ &= \overline{A \epsilon \sin(t)} \\ &= \overline{A + \epsilon_2 \sin(t) \epsilon \sin(t)} \end{aligned} \quad (2.14)$$

Thus, it is clear that we can move $\overline{\ddot{\theta}(t)}$ outside of the average value:

$$\overline{\dot{\phi} \dot{\theta} \sin 2\phi} = \mathbb{D} \overline{\ddot{\theta} \sin^2 \phi} \quad (2.15)$$

Finally, from Equation 2.12, we arrive at

$$\mathbb{C} = \theta^2 \overline{\ddot{\theta} \sin^2 \phi} (1 + \mathbb{D}) \quad (2.16)$$

Where $\mathbb{C} = \cos \bar{\phi}$. Since $\overline{f(\phi(t))} = f(\bar{\phi})$ as proven above, we finally prove that

$$\mathbb{C} = \theta^2 \overline{\ddot{\theta}} \mathbb{E} (1 + \mathbb{D}) \quad (2.17)$$

Which is

$$\theta^2 \bar{\theta} = \mathbb{K} \quad (2.18)$$

Where \mathbb{K} is some constant satisfying

$$\mathbb{K} = \frac{\mathbb{E}(1 + \mathbb{D})}{\mathbb{C}} \quad (2.19)$$

Thus, we can solve the differential equation

$$\bar{\theta} = \frac{\mathbb{K}}{\theta^2} \quad (2.20)$$

Solving the equation, we get that y equals to the solution of the equation:

$$\left(\frac{\mathbb{K} \log \left(-\mathbb{K} + \theta \mathbf{C}_1 + \sqrt{\mathbf{C}_1} \sqrt{\mathbf{C}_1 - \frac{2\mathbb{K}}{\theta}} \right)}{\mathbf{C}_1^{\frac{3}{2}}} + \frac{\theta \sqrt{\mathbf{C}_1 - \frac{2\mathbb{K}}{\theta}}}{\mathbf{C}_1} \right)^2 = (x + \mathbf{C}_2)^2 \quad (2.21)$$

Since Equation 2.21 is too complex to solve, the trial function $\theta = \alpha x^\beta$ is implemented and we get

$$(\beta - 1)\beta \alpha x^{\beta-2} = (\mathbb{K}\alpha)^{-2} x^{-2\beta} \quad (2.22)$$

From 2.22 we get

$$\begin{cases} (\beta - 1)\beta \alpha = (\mathbb{K}\alpha)^{-2} \\ \beta - 2 = -2\beta \end{cases} \quad (2.23)$$

Solving the system of equations 2.23, we get

$$\begin{cases} \alpha = \left(\frac{2}{9\mathbb{K}} \right)^{-\frac{1}{3}} \\ \beta = \frac{2}{3} \end{cases} \quad (2.24)$$

Which means that

$$\theta = \left(\frac{2}{9\mathbb{K}} \right)^{-\frac{1}{3}} t^{\frac{2}{3}} \quad (2.25)$$

To verify the solution, we can also approximate the problem as a simple conical pendulum problem, as shown in Fig.8, we can get:

$$m\omega^2 l \sin \phi = mg \tan \phi \quad (2.26)$$

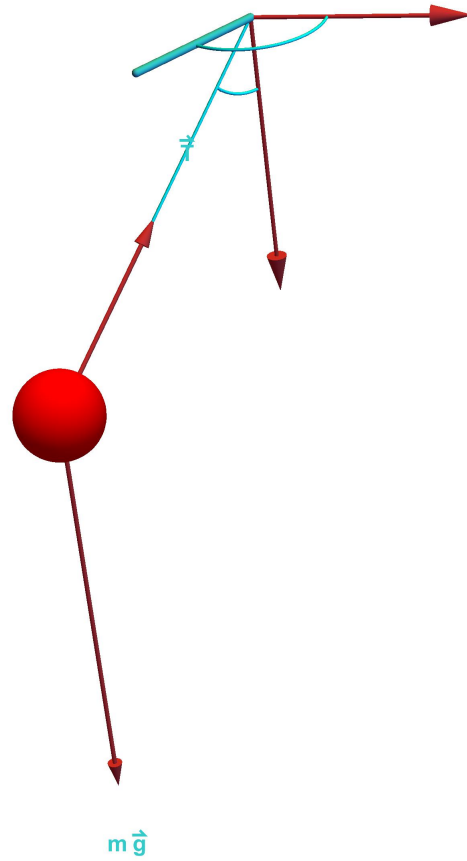


Figure 8 Free body diagram of the conical pendulum

Which is

$$\dot{\theta} = \sqrt{\frac{g}{l \cos \phi}} \quad (2.27)$$

By using the constraint condition $l = R\theta$, the relationship becomes:

$$\dot{\theta} = \sqrt{\frac{g}{R\theta \cos \phi}} \quad (2.28)$$

Where $\mathbb{L} = \sqrt{\frac{g}{R\theta}}$. Organize the equation, we can get a differential equation of the form:

$$\dot{\theta} = \frac{\mathbb{L}}{\theta^{\frac{1}{2}}} \quad (2.29)$$

We can solve this equation and get

$$\theta(t) = (3/2)^{\frac{2}{3}} (\mathbb{L}t + \mathbf{C})^{\frac{2}{3}} \quad (2.30)$$

From the initial condition

$$\theta(0) = 0 \tag{2.31}$$

We deduce that $\mathbf{C} = 0$, thus

$$\theta(0) = (3/2)^{\frac{2}{3}} (\mathbb{L}t)^{\frac{2}{3}} \tag{2.32}$$

Since in this approximated case, $\bar{\theta} = \theta$, $\bar{\dot{\theta}} = \dot{\theta}$, and $\bar{\ddot{\theta}} = \ddot{\theta}$, it is clear that when $t \gg 0$,

$$\begin{aligned} \theta &\propto t^{\frac{2}{3}} \\ \dot{\theta} &\propto t^{-\frac{1}{3}} \\ \ddot{\theta} &\propto t^{-\frac{4}{3}} \end{aligned} \tag{2.33}$$

These results can be verified using the numerical calculations done above. Fig.9 shows the result of a log-log plot of the function $\theta(t)$ and the linear best fit.

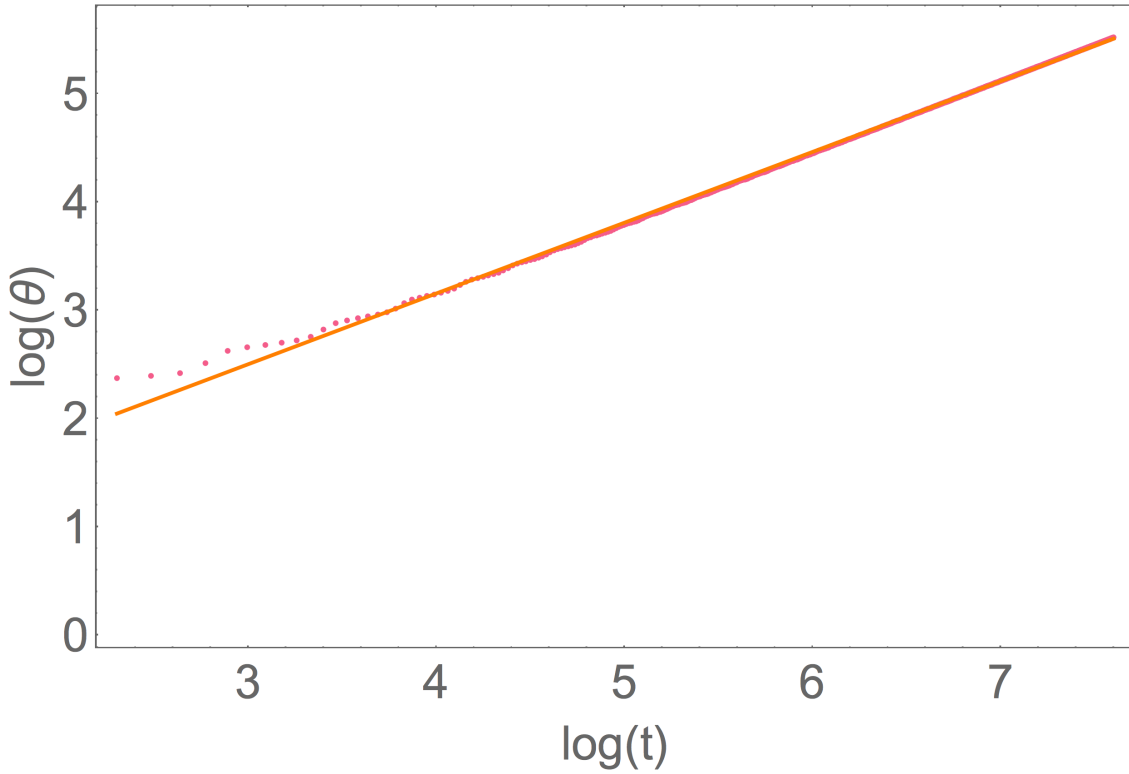


Figure 9 Linear fitting of the log-log plot

The result of the linear best fit is given as the following equations.

$$\theta = \alpha t^{\beta} \tag{2.34}$$

$$\log \theta = \beta \log t + \log \alpha \tag{2.35}$$

$$\begin{cases} \beta = 0.66 \approx \frac{2}{3} \\ \alpha = e^{1.77} = 5.88 \end{cases} \quad (2.36)$$

2.2.2 A Seemingly Paradoxical Problem

Something unexpected occur when proceeding the above calculations: the angular momentum of the system seems not being conserved, as shown in Fig.10.

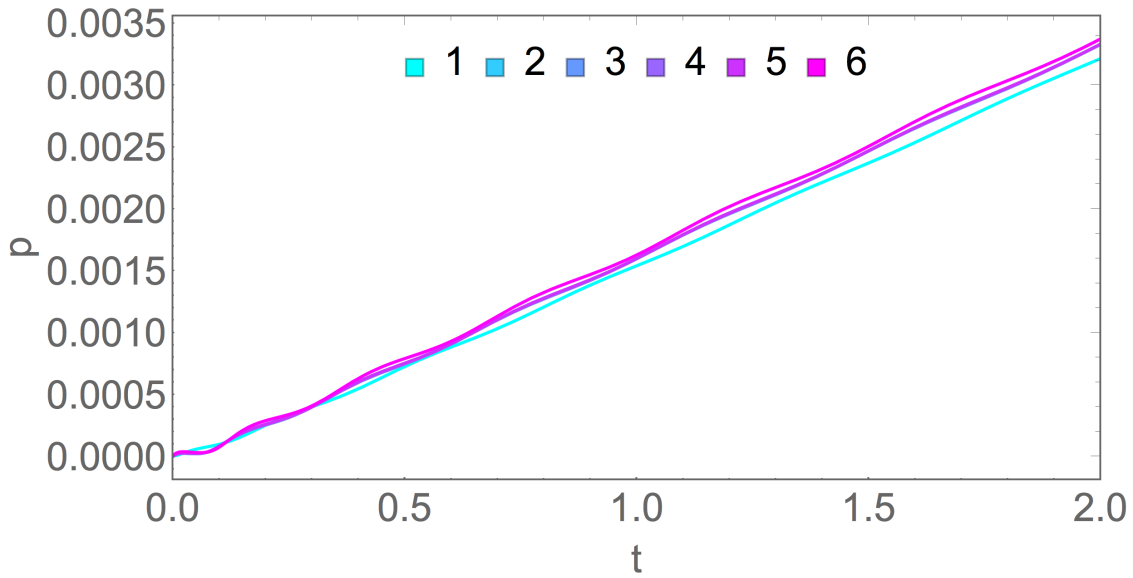


Figure 10 p v.s. t plot of the simulation

the plot of the angular momentum M versus time, which can also be verified from the fact that \mathcal{L} explicitly contains θ , thus

$$\frac{\partial \mathcal{L}}{\partial \theta} = m\dot{\phi}^2 R^2 \theta + gmR \cos \phi + mR^2 \theta \dot{\theta}^2 \sin^2 \phi \neq 0 \quad (2.37)$$

Since the model can be treated as a conical pendulum satisfying the condition $r \propto \theta$, the only external force should be the gravitational force and the tension on the rope.

This seemingly paradoxical problem can be explained since the simplified system is not necessarily conservative. The end of the rope is moving and the external tension force which keep the system obey the constrain conditions is doing work on the system.

Thus, the Lagrangian method couldn't be used in this problem.

However, this model can still be used as it is a relatively good approximation of the original problem when the time t is large enough, i.e. θ is large enough. Taking the $t \rightarrow \infty$ limit of the Lagrangian in Part 2.4, we can see that:

$$\begin{aligned} \lim_{t \rightarrow \infty} \left(\frac{1}{2}m(\dot{\phi}R\theta - R\dot{\theta} \sin \phi)^2 + \frac{1}{2}m(R\dot{\theta} - R\dot{\theta} \cos \phi)^2 + gmR\theta \cos \phi + \frac{1}{2}mR^2\theta^2\dot{\theta}^2 \sin^2 \phi \right) \quad (2.38) \\ = \frac{1}{2}m\dot{\phi}^2 R^2\theta^2 + \frac{1}{2}mR^2\dot{\theta}^2 + gmR\theta \cos \phi + \frac{1}{2}mR^2t^2\dot{\theta}^2 \sin^2 \phi \end{aligned}$$

2.3 Solution to the Original Problem

In the original question in Part 1.1, we have the following relationships:

$$T = \frac{2\pi}{\omega} \propto \omega^{-1} \quad (2.39)$$

$$n = \frac{\theta}{\pi} \propto \theta \quad (2.40)$$

Thus the problem becomes simply dealing with the following equation:

$$\dot{\theta} \propto \theta^{-\alpha} \quad (2.41)$$

Which is already shown in Part 2.4.1 that

$$\dot{\theta} \propto \theta^{-\frac{1}{2}} \quad (2.42)$$

Note that the result corresponds to that in the conical pendulum[4][5] as $l \gg 0$

$$\dot{\theta} = \sqrt{\frac{g}{R\theta \cos \phi}} \quad (2.43)$$

2.4 A Model involving the involute

2.4.1 The setup of the model

To simulate the phenomenon more accurately, Fig.11 and Fig.12 show the new model. Fig.11 gives out the Free body diagram of the forces acting on the bob and Fig.12 gives out the coordinates θ and ϕ .

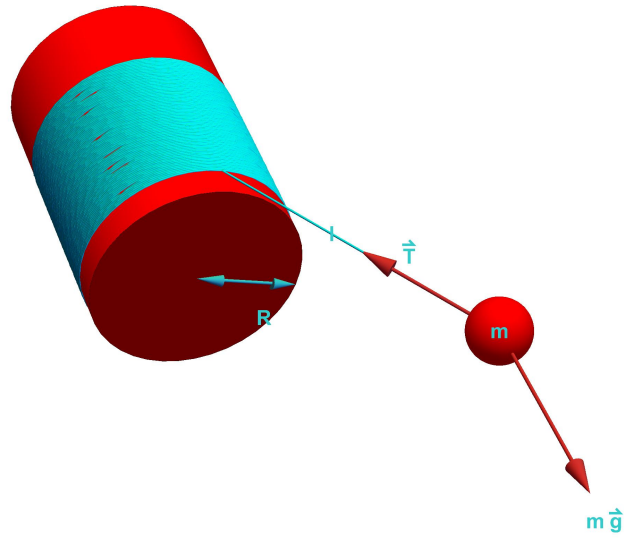


Figure 11 Free body diagram of the model

Taking the thickness of the pole into account, the motion of the bob is something similar to a so-called **involute** of a circle, which is the trajectory of the point tied to the circle with an imaginary string as the string is unwound from the circle.[6] We can get the new Lagrangian, as shown in Equation 2.44.

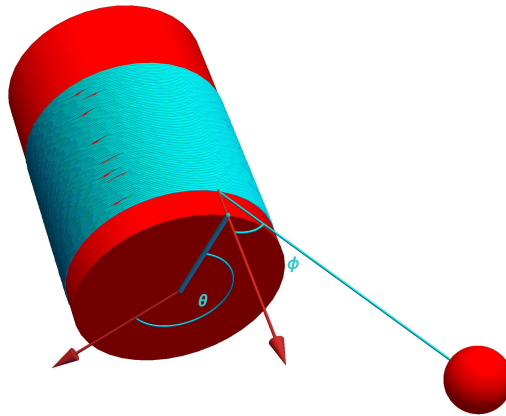


Figure 12 The two degrees of freedoms in the model

$$\mathcal{L} = gmR\theta \cos \phi + \frac{mR}{2}(\dot{\phi}\theta - \dot{\theta} \cos \phi)^2 + \frac{mR^2}{2}\theta^2\dot{\theta}^2 \sin^2 \phi + \frac{mR}{2}\dot{\theta}(1 - \sin \phi)^2 \quad (2.44)$$

Solving the Equations 2.5, which is, explicitly:

$$\begin{cases} -g \cos \phi + 2\dot{\phi}R\dot{\theta} + \ddot{\phi}R\theta + R(\sin \phi(\dot{\phi}^2\theta - 2\ddot{\theta}) + \dot{\phi}\theta^2\dot{\theta} \sin 2\phi + \sin^2 \phi(\theta^2\ddot{\theta} + \theta\dot{\theta}^2 + \ddot{\theta})) + \dot{\phi}^2 - \theta + \ddot{\theta}) + R\ddot{\theta} \cos^2 \phi = 0 \\ g \sin \phi - R \cos \phi(\theta\dot{\theta}^2 \sin \phi + \ddot{\theta}) + 2\dot{\phi}R\dot{\theta} + \ddot{\phi}R\theta = 0 \end{cases} \quad (2.45)$$

These equations can be solved numerically, and the change of θ through time is plotted, as shown in Fig 13.

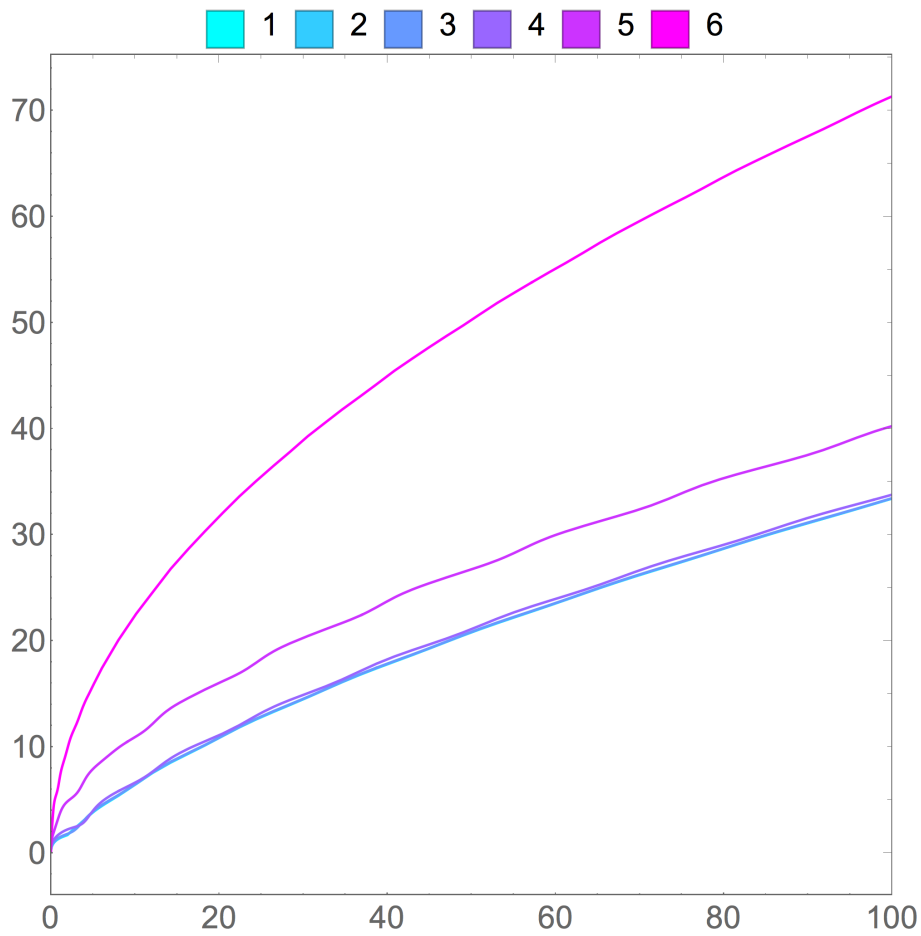


Figure 13 θ v.s. t plot.

The angle θ is monotonically increasing, and the angular velocity $\dot{\theta}$ is always greater than zero, which is reasonable due to the conservation of energy.

Since ϕ is more interesting to discuss, the following calculations used different sets of initial conditions as shown in Table 3, Table 4, Table 5, and Table 6. The results are collected and shown in Fig.14, Fig.15, Fig.16 and Fig.17.

Table 3 Initial conditions with different values of $\dot{\theta}_0$

$\dot{\theta}_0$	t	g	R	m	θ_0	$\dot{\theta}_0$	ϕ_0	$\dot{\phi}_0$
1	100	1	1	1	0.1	0	$\frac{\pi}{32}$	0
2	100	1	1	1	0.1	1	$\frac{\pi}{32}$	0
3	100	1	1	1	0.1	4	$\frac{\pi}{32}$	0
4	100	1	1	1	0.1	16	$\frac{\pi}{32}$	0
5	100	1	1	1	0.1	64	$\frac{\pi}{32}$	0
6	100	1	1	1	0.1	256	$\frac{\pi}{32}$	0

Table 4 Initial conditions with different values of ϕ_0

ϕ_0	t	g	R	m	θ_0	$\dot{\theta}_0$	ϕ_0	$\dot{\phi}_0$
1	100	1	1	1	0.1	10	$\frac{\pi}{64}$	0
2	100	1	1	1	0.1	10	$\frac{\pi}{32}$	0
3	100	1	1	1	0.1	10	$\frac{\pi}{16}$	0
4	100	1	1	1	0.1	10	$\frac{\pi}{8}$	0
5	100	1	1	1	0.1	10	$\frac{\pi}{4}$	0
6	100	1	1	1	0.1	10	$\frac{\pi}{2}$	0

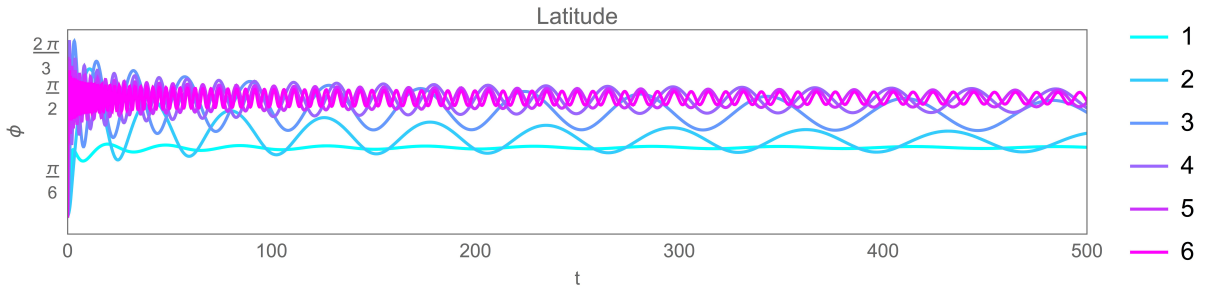


Figure 14 ϕ v.s. t plot with different values of $\dot{\theta}_0$

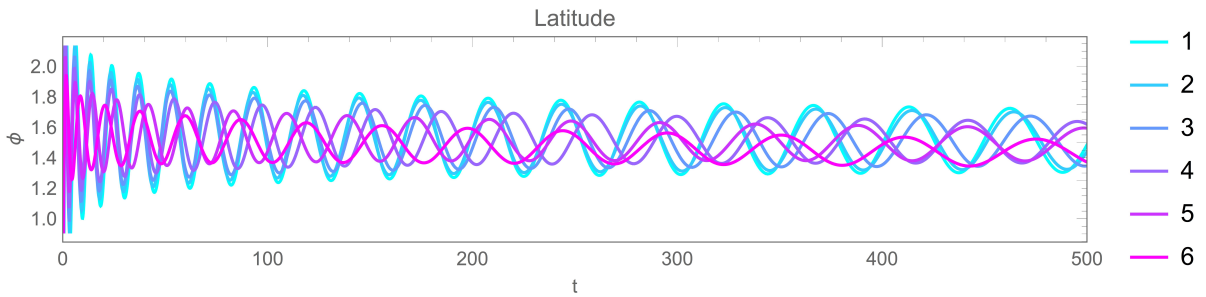


Figure 15 ϕ v.s. t plot with different values of ϕ_0

Table 5 Initial conditions with different values of $\dot{\phi}_0$

$\dot{\phi}_0$	t	g	R	m	θ_0	$\dot{\theta}_0$	ϕ_0	$\dot{\phi}_0$
1	100	1	1	1	0.1	10	$\frac{\pi}{32}$	0
2	100	1	1	1	0.1	10	$\frac{\pi}{32}$	1
3	100	1	1	1	0.1	10	$\frac{\pi}{32}$	2
4	100	1	1	1	0.1	10	$\frac{\pi}{32}$	4
5	100	1	1	1	0.1	10	$\frac{\pi}{32}$	8
6	100	1	1	1	0.1	10	$\frac{\pi}{32}$	16

Table 6 Initial conditions with different values of θ_0

θ_0	t	g	R	m	θ_0	$\dot{\theta}_0$	ϕ_0	$\dot{\phi}_0$
1	100	1	1	1	0.1	10	$\frac{\pi}{32}$	0
2	100	1	1	1	2.1	10	$\frac{\pi}{32}$	0
3	100	1	1	1	4.1	10	$\frac{\pi}{32}$	0
4	100	1	1	1	6.1	10	$\frac{\pi}{32}$	0
5	100	1	1	1	8.1	10	$\frac{\pi}{32}$	0
6	100	1	1	1	10.1	10	$\frac{\pi}{32}$	0

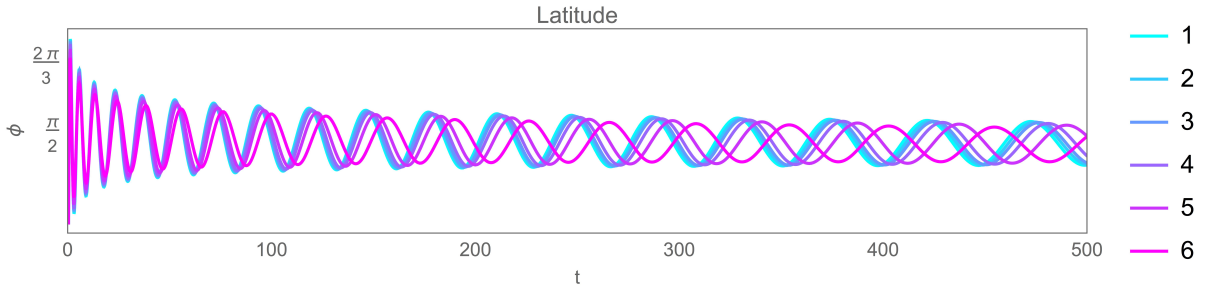


Figure 16 ϕ v.s. t plot with different values of $\dot{\phi}_0$

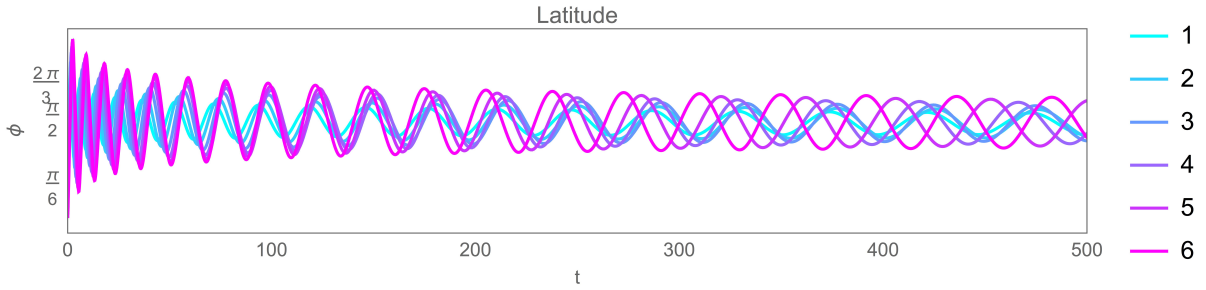


Figure 17 ϕ v.s. t plot with different values of θ_0

Apparently, the latitudinal angle tends to some fixed number[7] as time tends to infinity, this number doesn't depend on θ_0 or $\dot{\phi}_0$ and is further discussed in Part 2.4.3.

2.4.2 Final results of the simulation

Using the calculated result in Part 2.4, a parametric plot corresponding to the overview of the trajectory of the pendulum bob can be done. The mathematical formulation of the plot is:

$$\begin{cases} x = R \cos \theta + \theta R \sin \theta \sin \phi \\ y = R \sin \theta - \theta R \cos \theta \sin \phi \end{cases} \quad (2.46)$$

Whereas the involute of a circle, Equation 2.47 is also plotted for comparison in Fig.18, Fig.19, Fig. 20, and Fig.21.

$$\begin{cases} x = R \cos \theta + \theta R \sin \theta \\ y = R \sin \theta - \theta R \cos \theta \end{cases} \quad (2.47)$$

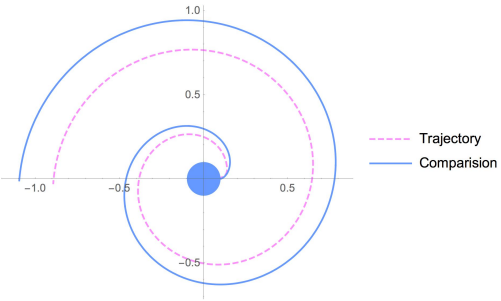


Figure 18 Trajectory top view, $t = 0 \dots 2$

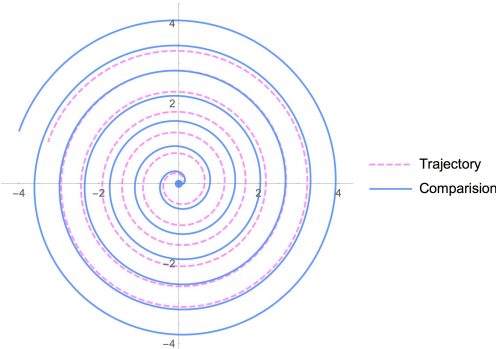


Figure 19 Trajectory top view, $t = 0 \dots 50$

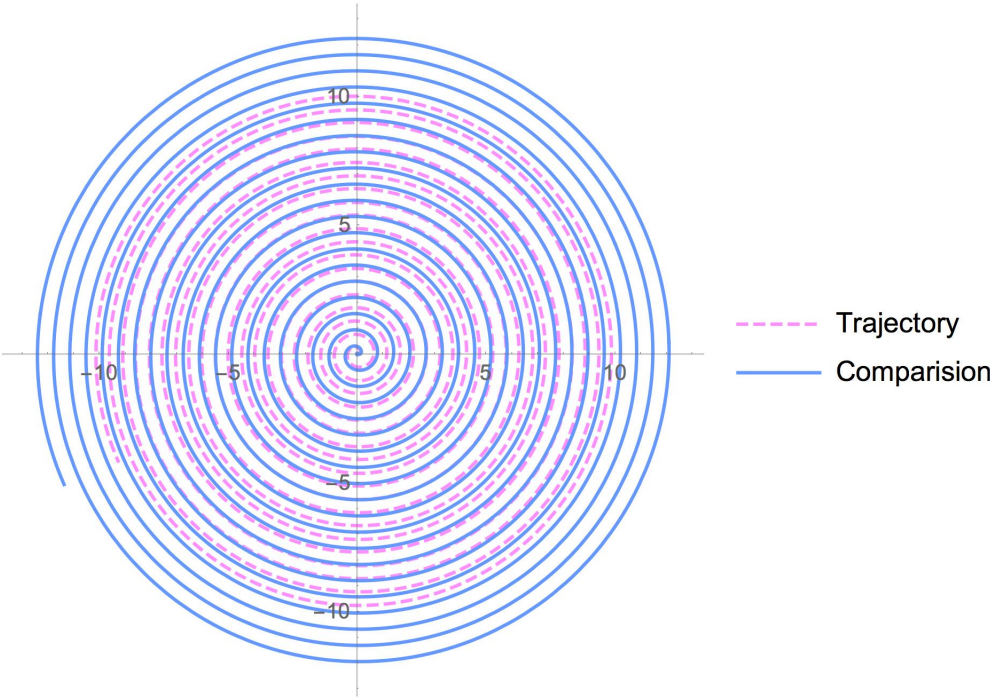


Figure 20 Top view of trajectory with $t = 0 \dots 200$

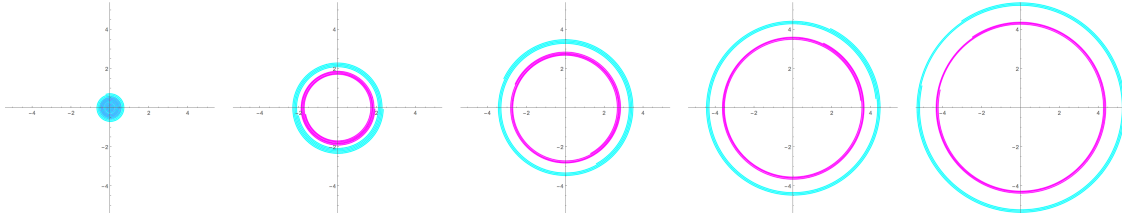


Figure 21 Trajectory with comparison involute of a circle in different instances

To make the changing of the angle ϕ clear, a side-view plot can also be done parametrically by calculating $l \sin \phi$ and $l \cos \phi$, as shown in Fig.22 and Fig.23.

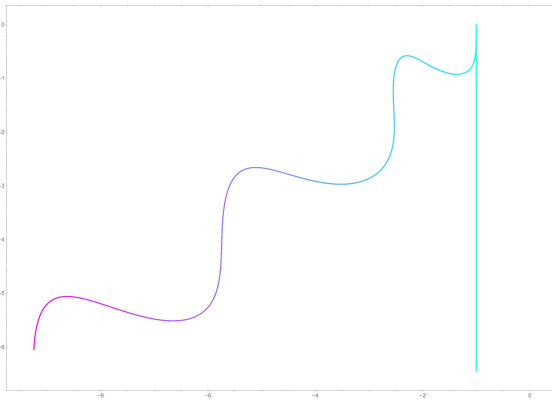


Figure 22 Trajectory side view, $t=0 \dots 2$

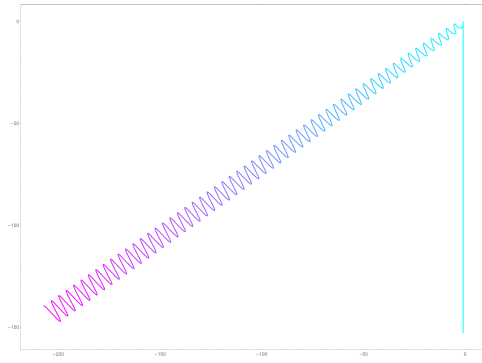


Figure 23 Trajectory side view, $t=0 \dots 200$

These graphs give us an interesting insight that though the amplitude of oscillation of ϕ , A_ϕ , is gradually decaying towards zero, the actually longitudinal oscillation, namely lA_ϕ is actually increasing since

$$lA_\phi = R\theta A_\phi$$

A 3D graph can also be plotted parametrically and shown in Fig.24 and Fig.25.

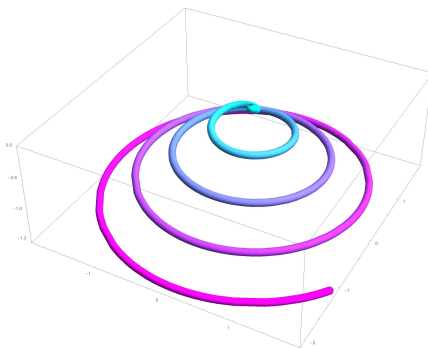


Figure 24 3D parametric plot with $t = 0 \dots 10$

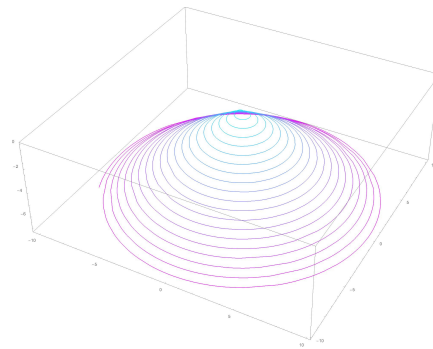


Figure 25 3D parametric plot with $t = 0 \dots 200$

2.4.3 Discussion of the possible values of ϕ

It is interesting that the ϕ angle tends to a certain value regardless of initial conditions. In this paragraph, we will illustrate this phenomenon more quantitatively[8][9].

The mechanical energy is conserved since the pole doesn't do work on the rope and the rope is gradually unwound in a involute motion. Alternatively, this can be also seen from the time independence of the Hamiltonian[10]:

$$\begin{aligned}\mathcal{H} &= \sum_{i=1}^n q_i p_i - \mathcal{L} \\ &= \frac{1}{2}m(\dot{\phi}R\theta - R\dot{\theta} \sin^2 \phi) + \frac{1}{2}m(R\dot{\theta} - R\dot{\theta} \cos^2 \phi) - gmR\theta \cos \phi + \frac{1}{2}mR^2\dot{\theta}^2 \sin^2 \phi\end{aligned}\quad (2.48)$$

Where $\frac{\partial \mathcal{H}}{\partial t} = 0$. Thus, the total energy equals to the initial energy:

$$E_0 = gmR\theta_0 \cos \phi_0 + \frac{mR}{2}(\dot{\phi}_0\theta_0 - \dot{\theta}_0 \cos \phi_0)^2 + \frac{mR^2}{2}\dot{\theta}_0^2 \sin^2 \phi_0 + \frac{mR}{2}\dot{\theta}_0(1 - \sin \phi_0)^2 \quad (2.49)$$

In a macroscopic view, the model can be approximated to a spherical pendulum[11], i.e. a point of mass with mass m , subjected to a vertically placed gravitational field and constraint to move only in a sphere of radius l .

The effective potential, U_{eff} can be calculated with the following steps, since the Lagrangian of a spherical pendulum is:

$$\frac{ml^2\dot{\theta}}{2} + \frac{1}{2}ml^2 \sin^2 \theta \dot{\phi}^2 - mgl \cos \theta \quad (2.50)$$

Thus, by dropping the kinetic energy term $\frac{ml^2\dot{\theta}}{2}$, we can spot that the effective potential U_{eff} .

$$U_{eff} = \frac{1}{2}ml^2 \sin^2 \theta \dot{\phi}^2 - mgl \cos \theta \quad (2.51)$$

The range of motion of the angle ϕ can be made clear by the boundary condition $E > U_{eff}$, whose boundary is determined by the equation $E = U_{eff}$, which is explicitly:

$$E = \frac{1}{2}ml^2 \dot{\phi}^2 \sin^2 \theta - mgl \cos \theta \quad (2.52)$$

This is a quadratic equation and will have at most two solutions, which determine the upper and lower bounds of the angle ϕ . Using the substitution $x = \cos \phi$ and solving

Equation 2.52, we can get two solutions:

$$\begin{cases} x_1 = -\frac{gm + \sqrt{m(g^2m - 2E\dot{\theta}^2 + l^2m\dot{\theta}^4)}}{lm\dot{\theta}^2} \\ x_2 = \frac{-gm + \sqrt{m(g^2m - 2E\dot{\theta}^2 + l^2m\dot{\theta}^4)}}{lm\dot{\theta}^2} \end{cases} \quad (2.53)$$

Taking the limit $l \rightarrow \infty$, we can get

$$\begin{cases} x_1 = -1 \\ x_2 = 1 \end{cases} \quad (2.54)$$

It is obvious that the angle ϕ would not exceed the range $(0, \pi)$ regardless of the initial conditions. Now, to be more accurate, we should take the change of l in to account by simply plugging in the relationships 2.55 we have proven above:

$$\begin{aligned} \theta &= kt^{\frac{2}{3}} \\ \dot{\theta} &= \frac{2}{3}kt^{-\frac{1}{3}} \end{aligned} \quad (2.55)$$

Where k is a constant satisfying $k = \left(\frac{3}{2}\right)^{\frac{2}{3}} \mathbb{L}$ and L is the constant that can be determined from Equation 2.29. We can get:

$$\begin{cases} x_1 = \frac{-9mg + \sqrt{16m^2k^6R^2 + 81m^2g^2 - 72mEk^2t^{-\frac{2}{3}}}}{4k^3mR} \\ x_2 = \frac{-9mg + \sqrt{16m^2k^6R^2 + 81m^2g^2 - 72mEk^2t^{-\frac{2}{3}}}}{4k^3mR} \end{cases} \quad (2.56)$$

Taking the limit $t \rightarrow \infty$, we can get:

$$\begin{cases} x_1 = \frac{-9g - \sqrt{16k^6R^2 + 81g^2}}{4k^3R} \\ x_2 = \frac{-9g + \sqrt{16k^6R^2 + 81g^2}}{4k^3R} \end{cases} \quad (2.57)$$

which gives the upper and lower bounds of ϕ .

2.5 Model of the original problem

The original model of the **Danza de los Voladores** includes four identical pendula connected to a spinning square platform. Some minor modifications, including the kinetic energy of the spinning platform should be taken into account, as shown in Fig.26.

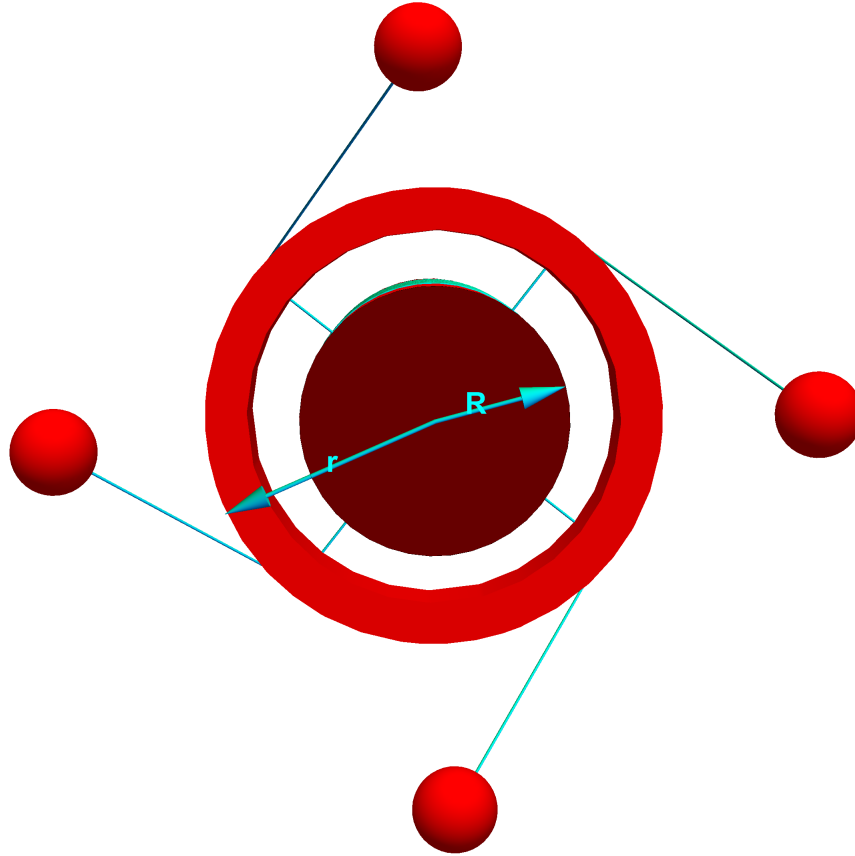


Figure 26 Bottom view of the platform

The new Lagrangian is:

$$\mathcal{L} = 4gmR\theta \cos \phi + I\dot{\theta}^2 + 2mR^2(\dot{\phi}\theta - \dot{\theta} \sin^2 \phi) + 2mR^2\theta^2\dot{\theta}^2 \sin^2 \phi + 2mR^2\dot{\theta}(1 - \cos \phi)^2 \quad (2.58)$$

Where I is the moment of inertia of the platform. This modification doesn't affect much on the original problem, where the mass is simply multiplied by a factor of 4 and the effect of the term $I\dot{\theta}^2$ will be insignificant when $2mR^2\theta^2 \gg I$. Thus, the **Involute model** in Part 2.4 can give a relatively accurate prediction of the motion.

3 Experiments

3.1 Overview

In this session, the experiments are carried out to verify the theoretical model and to offer a direct observation of the phenomenon. The motion of the winding pendulum is created and the data of seven separate trials are extracted. The data are then analyzed with computer to verify the theoretical model. Finally, a short discussion about the sudden-sliding problem of the thread is discussed.

3.2 Experiment setup

To achieve the goal, common daily materials, such as paper towel roll, light bulb, woolen thread, printing paper, glue and scale weights are used to create the dynamic system, as shown in Fig.27. Torches and slow motion cameras are used to keep track of experimental data where as computational programs are employed for data processing and analysis of the results.



Figure 27 Materials used in the experiment

In order to explore the effect of different R and m , a set of scale weights and poles with various radii are used. To possibly reduce the effect of friction between the pole and the thread, poles with different materials are utilized.

The pole is fixed on a stand over a table such that the pendulum can swing freely, as shown in Fig.28. Two slow motion cameras are set up directly below and beside the pole respectively to trace the angle θ and ϕ .



Figure 28 Experimental setup

Using this method, seven sets of data are gathered, including the time dependency of θ and ϕ . The initial conditions of the coordinates: ϕ , ϕ_0 , θ , and θ_0 can be approximated by their respective calculated values at the very beginning of the releases.

3.2.1 Trial 1&2

For convenience, experimental data was extracted from the video manually by locating points of motion in different instances using a Mathematica locator program. The extracted plots are shown in the following figures.

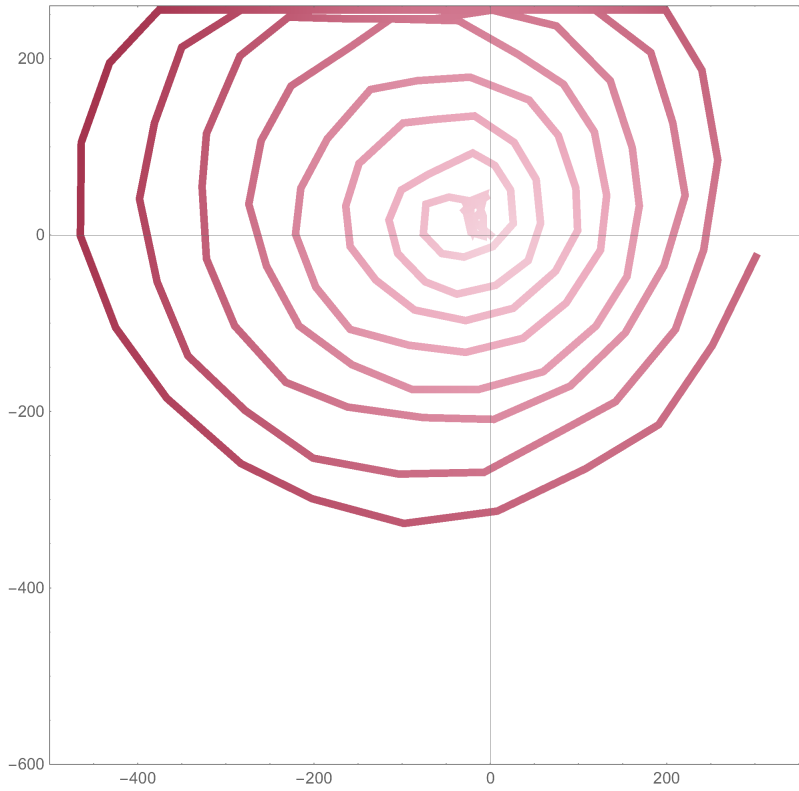


Figure 29 Trajectory of the bob in Trial 1

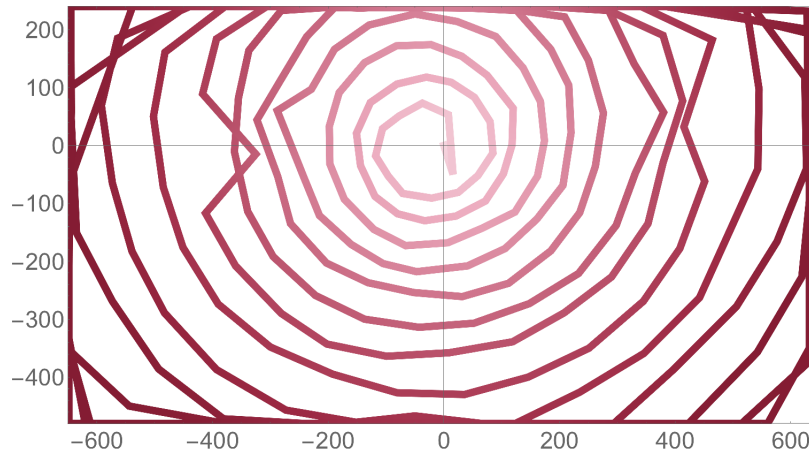


Figure 30 Trajectory of the bob in Trial 2

A simple calculation $\phi = \arctan \frac{y}{z}$ is done and a program is implemented to ensure the monotonic increasing of the function (due to the none subjectivity of the arctan function), from which we get the change of ϕ over time, which is plotted as follows:

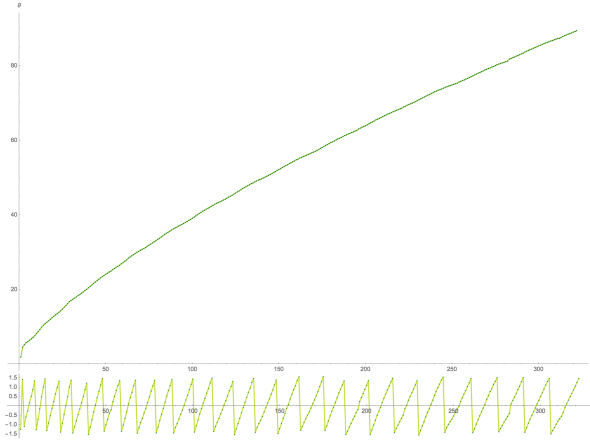


Figure 31 ϕ v.s. t plot of trial 1

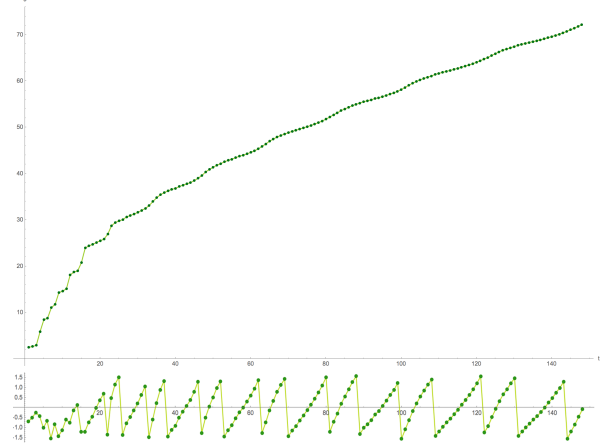


Figure 32 ϕ v.s. t plot of trial 2

A initial observation clearly indicates the decaying oscillation of the ϕ coordinate through time and θ with changing slope, which exactly matches the predicted phenomenon. On the other hand, in a larger time scale, the motion shows a decay in angular velocity, mainly due to the effects of the non-conservative forces. To verify the ratio relationship of θ , $\dot{\theta}$ and time, the data can be converted to a log-log scale and a linear fit is done to determine the coefficients α and β .

The plot of the linear fitting function and the original data is shown in Fig.33 and Fig.34.

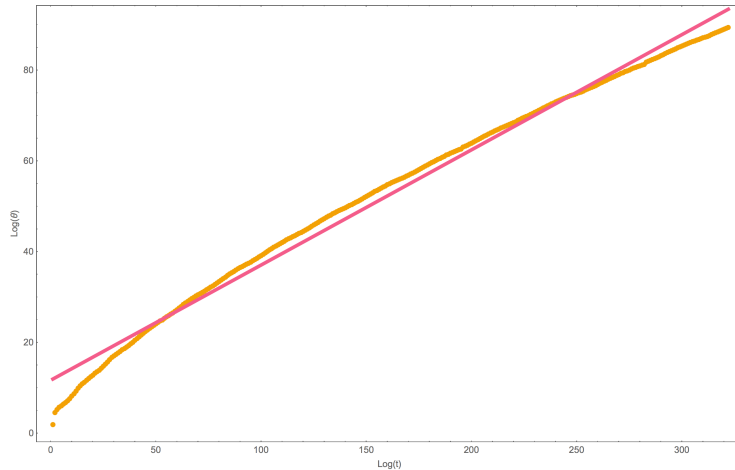


Figure 33 Linear fit of the log-log plot 1

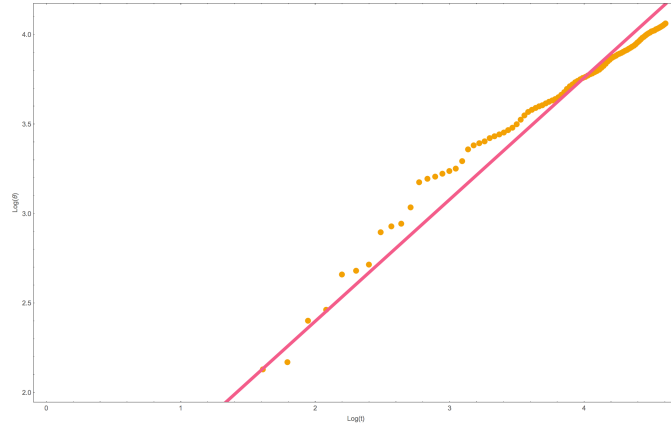


Figure 34 Linear fit of the log-log plot 2

The calculated values of α and β are, respectively

$$\begin{cases} \beta = 0.67 \approx \frac{2}{3} \\ \alpha = e^{0.58} = 5.88 \end{cases} \quad (3.1)$$

$$\begin{cases} \beta = 0.68 \approx \frac{2}{3} \\ \alpha = e^{0.58} = 1.03 \end{cases} \quad (3.2)$$

3.2.2 Trial 3-7

In order to obtain more accurate results, a light is attached to the bob and the bob is re-weighted to compensate the possible errors as shown in Fig.35. Then, videos are recorded in slow motion with the frames extracted and analyzed using MATLAB. By locating the pixel with the greatest intensity, the data of the bob's position can be extracted from the video. The value of the constant R can be simply determined by counting the pixels as shown in Fig.36.

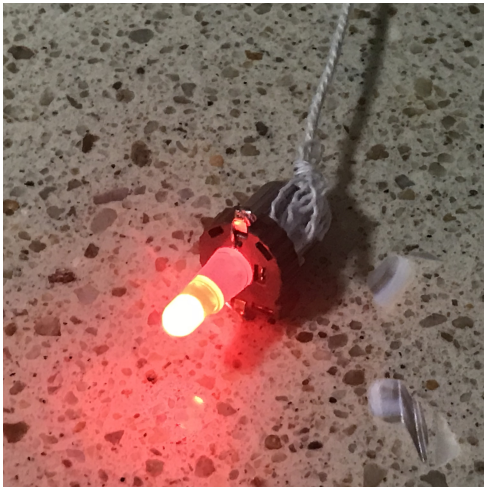


Figure 35 The light used to trace the position of the bob



Figure 36 The way to determine R

Table 7 shows the conditions of the experiment.

Table 7 The conditions of the experiment

Variables	g	R	m	θ_0	$\dot{\theta}_0$	ϕ_0	$\dot{\phi}_0$
Values	9.8	0.01	0.01	$\frac{\pi}{2}$	0	$\frac{\pi}{4}$	0

After the slow-motion videos are recorded, the frames are extracted from the video. Binarization and image-addition are processed to provide a more intuitive view of the coordinates' relative changes, which are shown in Fig.37 and Fig.38.



Figure 37 Trial 3 Overview

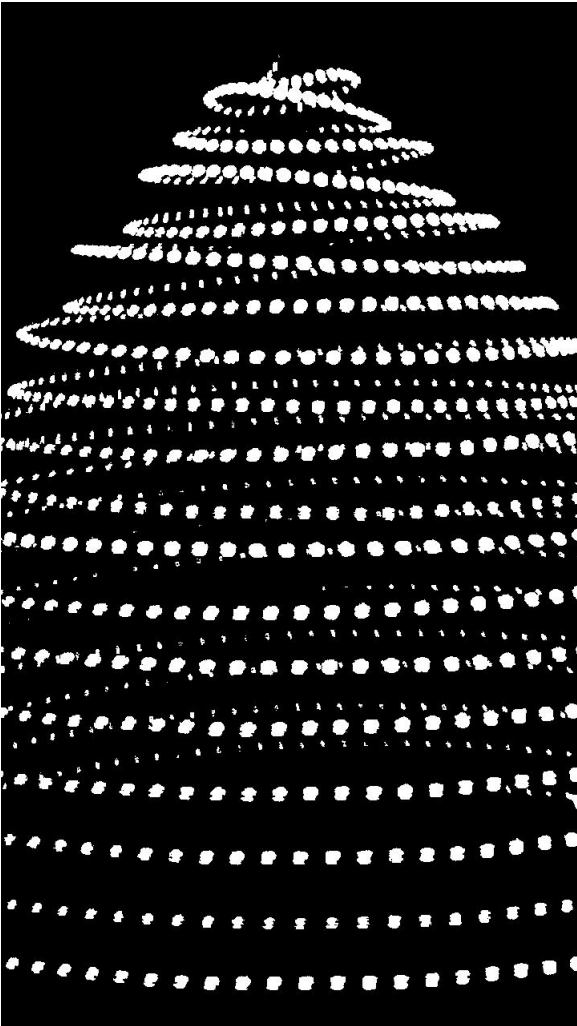


Figure 38 Trial 3 Sideview

The largest experimental errors are caused by the limit of the visual angle of the camera, which gives rise to the times when the bob is out of the edge of the recording window. When nothing is present in the range losing track of the bob, the program will generate much noise, as shown in the following graphs.

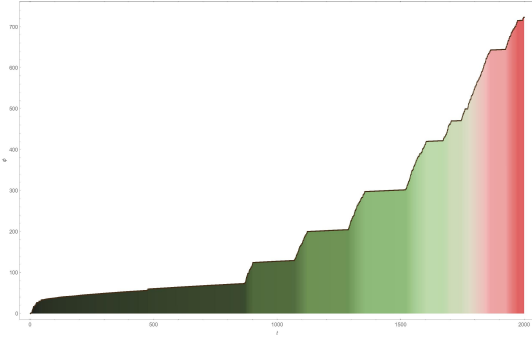


Figure 39 Trial 3 θ with noise

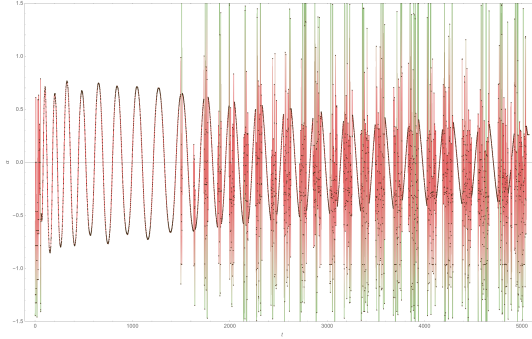


Figure 40 Trial 3 α with noise

A filtering program, as attached in the appendix, is implemented to reduce the noise. The results are shown in Fig.41 and Fig.42.

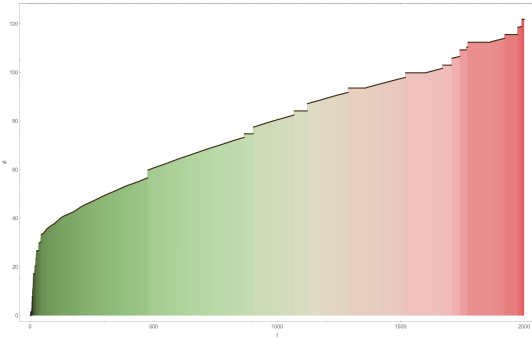


Figure 41 Trial 3 θ with noise reduced

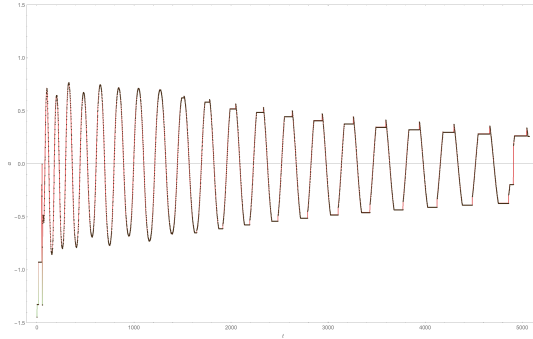


Figure 42 Trial 3 α with noise reduced

The filtrated data of motion in trials 3-7 are shown in Fig.43 and Fig.44, respectively.



Figure 43 The overview data of motion of five trials 3-7

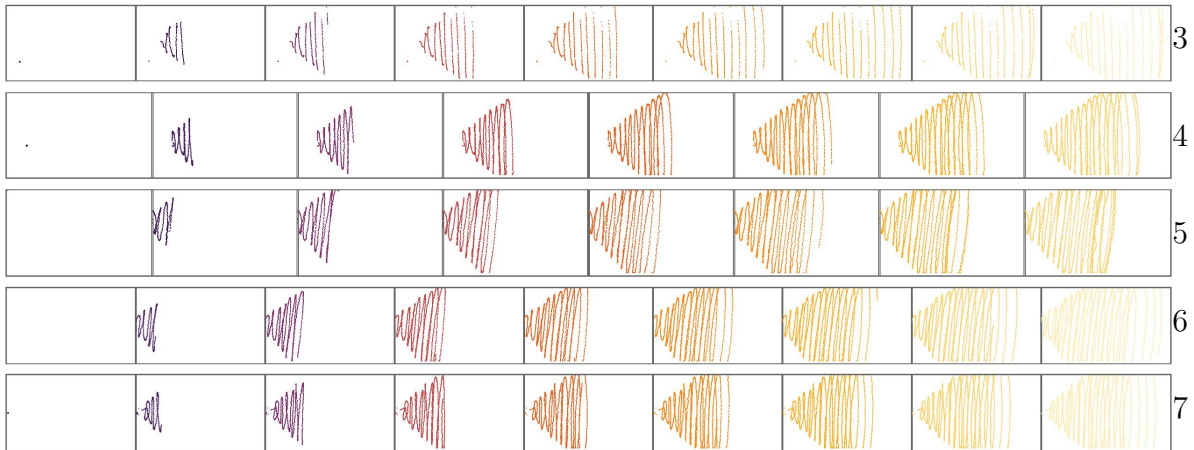


Figure 44 The side-view data of motion of trials 3-7

3.2.3 About the sliding problem

A strange phenomenon occurs during the experiment, as highlighted in Fig.45. If the radius R is large and the initial angular velocities $\dot{\theta}$ and ϕ are comparatively small, the rope will display a rapid unwinding and sliding around the pole accompanied with the bob falling directly to the ground.



Figure 45 Photographs of the sudden-sliding phenomenon

A possible explanation can be given to interpret the cause of this phenomenon. The tension on the string can be calculated through the method of Lagrangian multiplier with the following procedure.

Introduce a new coordinate l , the length of the rope which satisfies the constraint relationship $l = R\theta$, i.e. $f(l, R) = l - R\theta = 0$. By introduce the Lagrangian multiplier λ , we can get the following equations of motion:

$$\begin{cases} \frac{d}{dt} \frac{\partial \mathcal{L}}{\partial \dot{\theta}} = \frac{\partial \mathcal{L}}{\partial \theta} - \lambda R \\ \frac{d}{dt} \frac{\partial \mathcal{L}}{\partial \dot{\phi}} = \frac{\partial \mathcal{L}}{\partial \phi} \\ \frac{d}{dt} \frac{\partial \mathcal{L}}{\partial \dot{l}} = \frac{\partial \mathcal{L}}{\partial l} + \lambda \\ l - R\theta = 0 \end{cases} \quad (3.3)$$

From the first equation, we can get the relationship:

$$\begin{aligned} \lambda = T &= \frac{ml}{R} \sin \phi (2\dot{l}\dot{\theta} \sin \phi + l(2\dot{\theta}\dot{\phi} \cos \phi + \ddot{\theta} \sin \phi)) \\ &= m\theta \sin \phi (2R\dot{\theta}^2 \sin \phi + R\theta(2\dot{\theta}\dot{\phi} \cos \phi + \ddot{\theta} \sin \phi)) \end{aligned} \quad (3.4)$$

which gives out the relationship between the quantity of motions and the tension on the string. On the other hand, during the unwinding process, the rope is not necessarily horizontally wound on the pole, but with some tilting angle instead. This makes the point of contact between the pole and the thread a part of an ellipse, in the zoomed

experiment picture (Fig.46). The curvature radius ρ satisfies:

$$\rho = \frac{b^2}{a} = \frac{R^2 \csc \phi}{R} = R \csc \phi \quad (3.5)$$

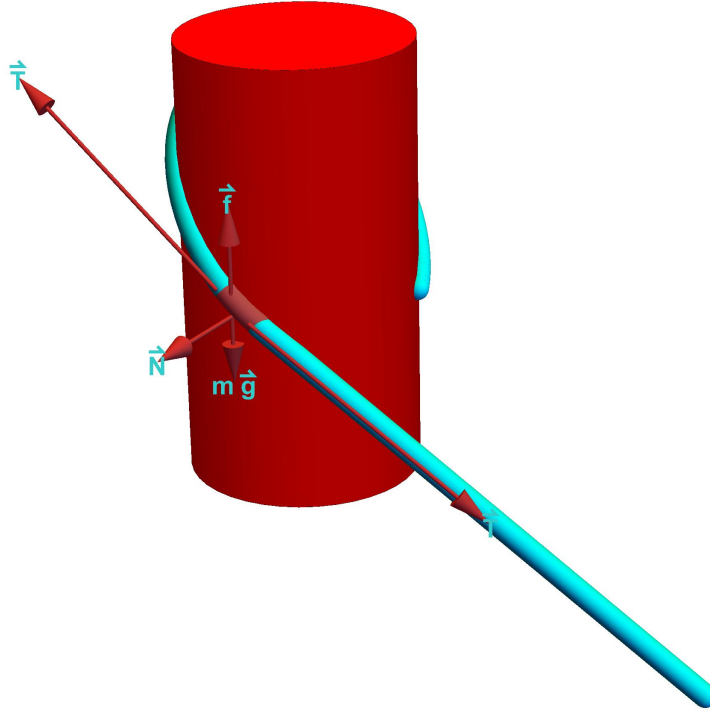


Figure 46 Zoomed diagram of the thread

Thus, suppose the line mass of the rope is σ , for a small piece of rope with length dl , the following calculations can be done to get the relationship between these quantities.

$$\frac{d\theta}{2} 2T = dN = \frac{df}{\mu} \quad (3.6)$$

To avoid sliding, the following inequality should hold.

$$gdm < df \leq \mu T d\theta \quad (3.7)$$

$$g\sigma dl \leq \mu T \frac{dl}{R} \quad (3.8)$$

Thus, simplify the relation, we can get:

$$g\sigma \leq \mu \frac{T}{\rho} \tag{3.9}$$

Since $\rho = R \csc \phi$ holds as shown in Fig.3.2.3, we have

$$g\sigma \leq \mu \frac{T}{R \csc \phi} \tag{3.10}$$

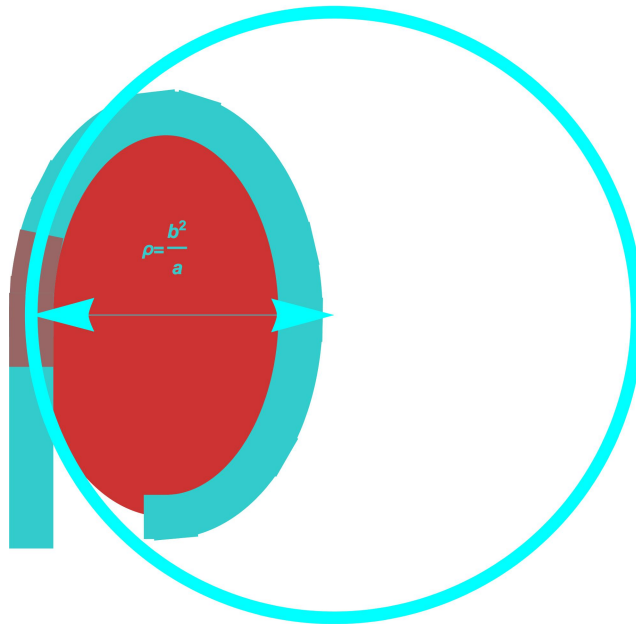


Figure 47 Relationship between rhp , a and b

Therefore, it is clear that why the radius of the pole should not be too large and the rope should not be too heavy in order to recreate the phenomenon.

However, in the **Danza de los Voladores**, due to the existence of the platform, this phenomenon won't occur. The platform's own moment of inertia ensures a relatively big value of the tension on the string, whereas the edge of the platform also serves as pulleys, changing the direction of the tension and making the tangent point vertical to the surface of the pole. The ropes are also thick enough to ensure that lower ropes give upper ropes normal force at the beginning of the motion. All of these conditions reduce the possibility of the occurrence of this sudden-sliding phenomenon and make the performance a much safer activity.

3.3 Data Analysis

3.3.1 Collection of the data

The longitudinal (azimuthal) angle is relatively simple to extract, and the change of θ in the five trials is plotted and shown in Fig.48.

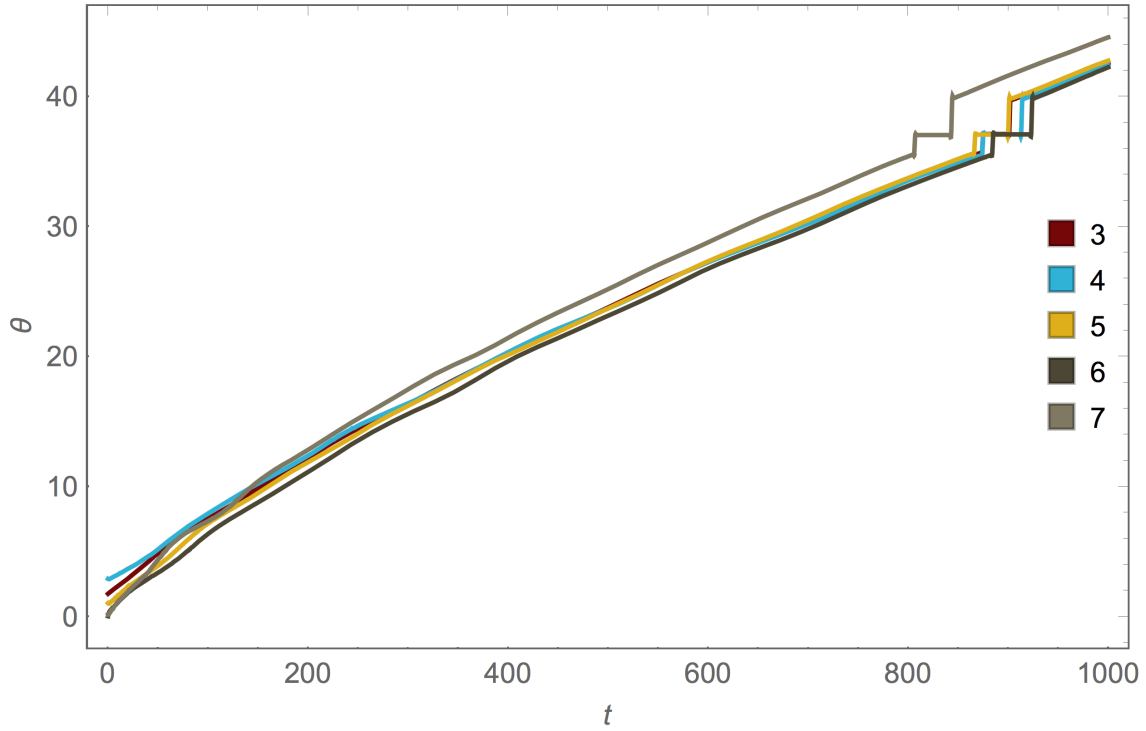


Figure 48 The changing of θ over time

To determine the latitude, an auxiliary angle, namely α and an auxiliary length τ are used, which are defined as the diagram shown below (Fig.49).

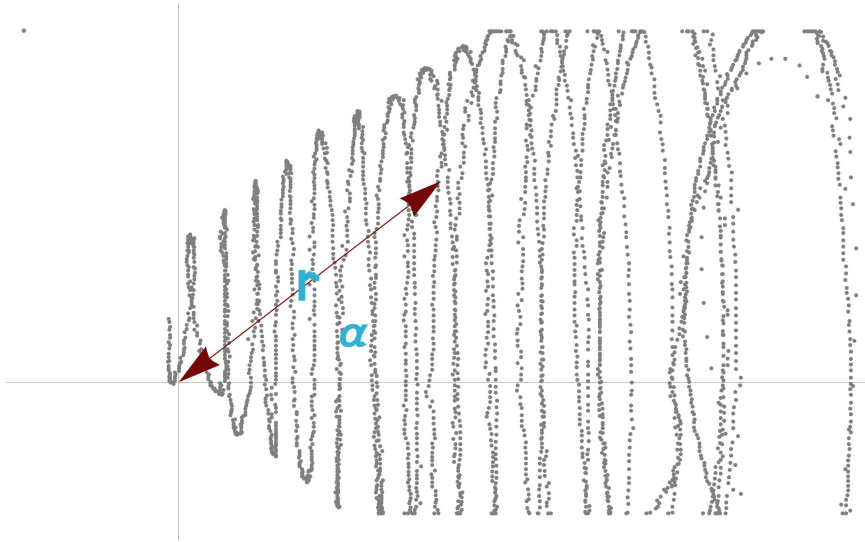


Figure 49 The definition of α , τ

These quantities can be extracted respectively by Mathematica programs. The results of the five trails are plotted and shown in Fig.50, respectively.

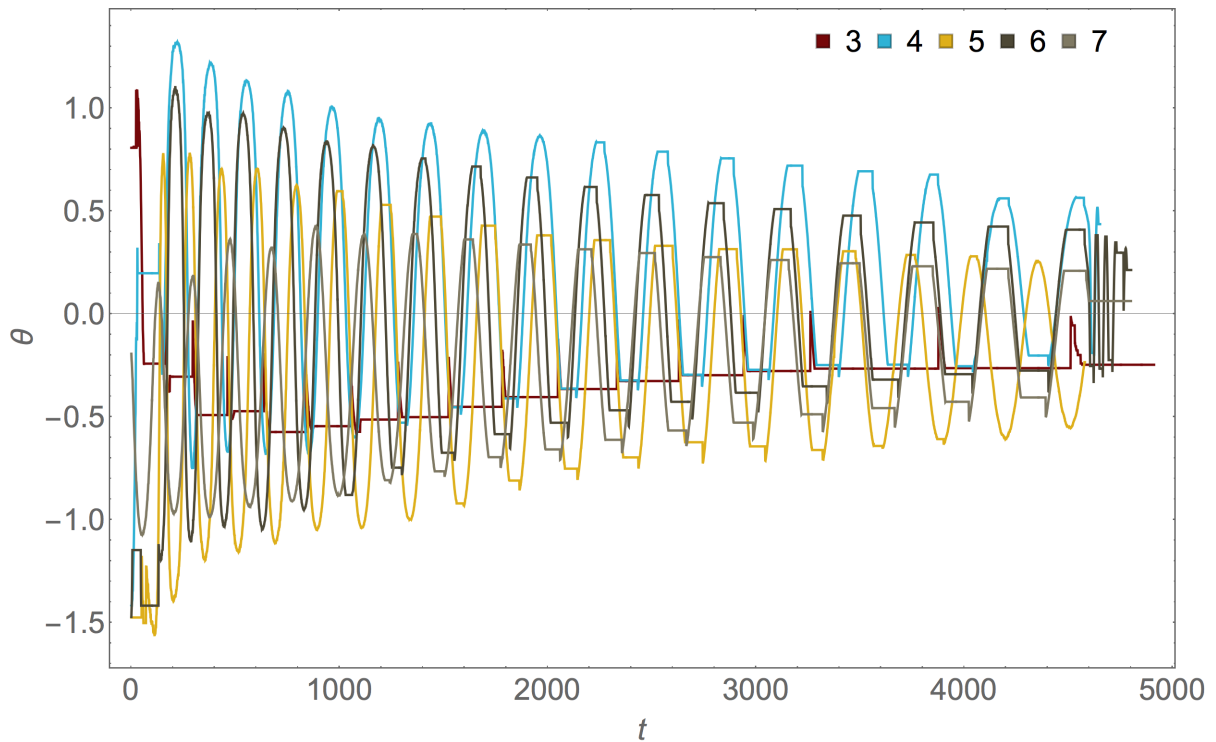


Figure 50 The changing of α over time

The latitude can now be extracted in two ways, namely, using the constraint relation-

ship and the measured rope length from bottom to determine the value of $\sin \phi$, thus determining ϕ . By using the equation

$$\theta = \arctan \left(\frac{l \sin \phi \sin \theta}{l \cos \phi} \right) = \arctan \left(\frac{\tan \alpha}{\sin \theta} \right) \quad (3.11)$$

Alternatively, it is possible to measure ϕ directly at a fix position of loop, and convert the time scale with the already-known function $\theta(t)$, by using

$$\begin{aligned} l \cos \phi &= r \cos \alpha \\ \Rightarrow \phi &= \arccos \left(\frac{r \cos \alpha}{l} \right) \end{aligned} \quad (3.12)$$

For a better program performance, the data extracting is confined in one visual angle, which is the top view one. The ϕ v.s. t plots of trials 3-7 are done below in Fig.51.

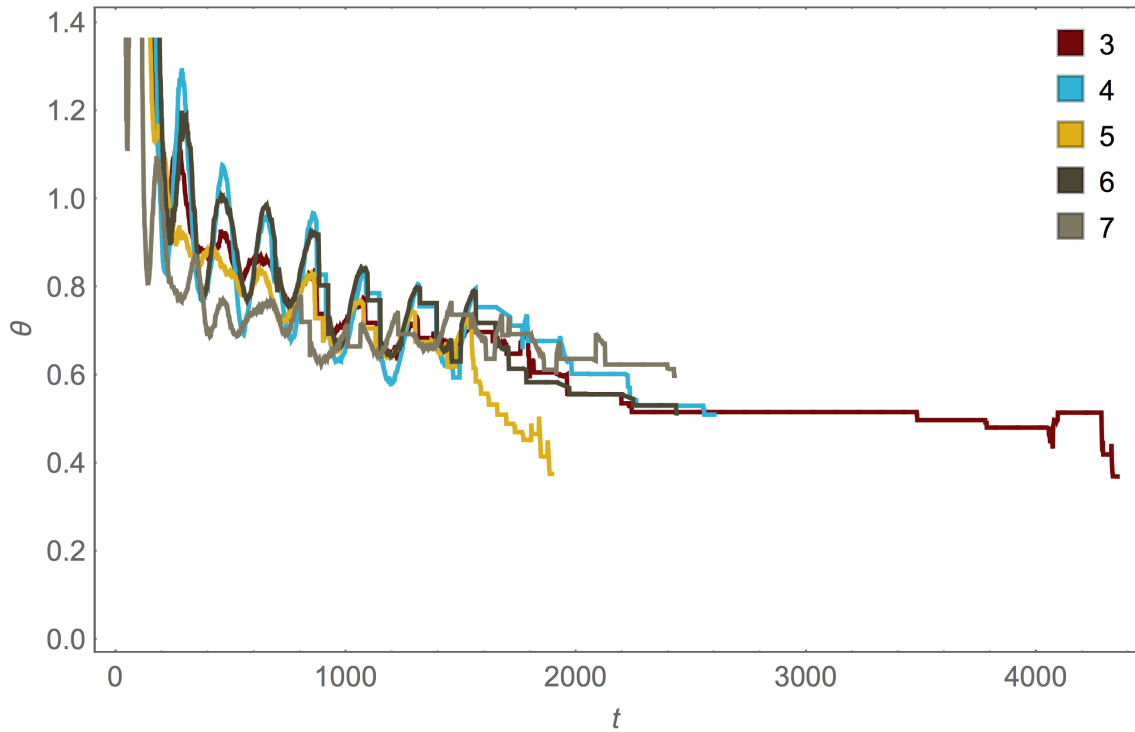


Figure 51 The changing of ϕ over time

A Mathematica program is used (as shown in the Appendix) to convert the coordinates, interpolate the points and numerically differentiate the interpolation function for $\dot{\theta}$, $\dot{\phi}$, $\ddot{\theta}$ and $\ddot{\phi}$, which are then plotted as shown in Fig.52, Fig.53, Fig.54, and Fig.55 below.

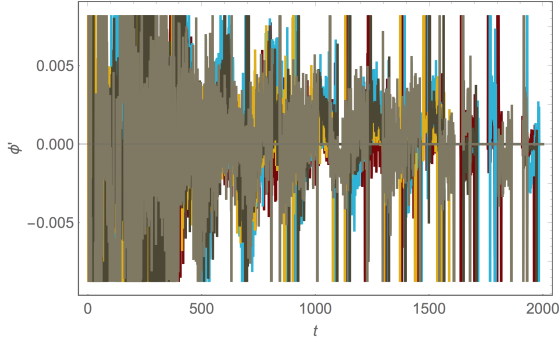


Figure 52 $\dot{\phi}$ v.s. t of five trials

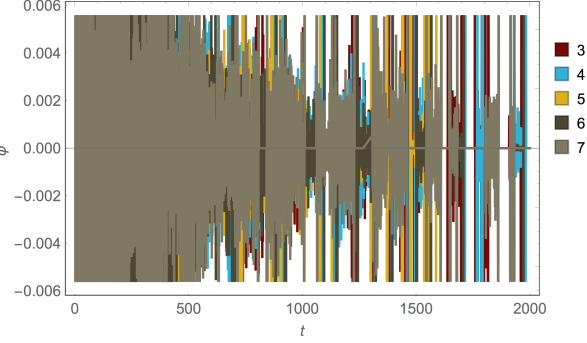


Figure 53 $\ddot{\phi}$ v.s. t of five trials

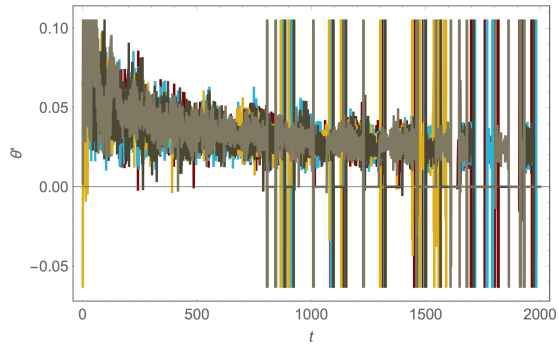


Figure 54 $\dot{\theta}$ v.s. t of five trials

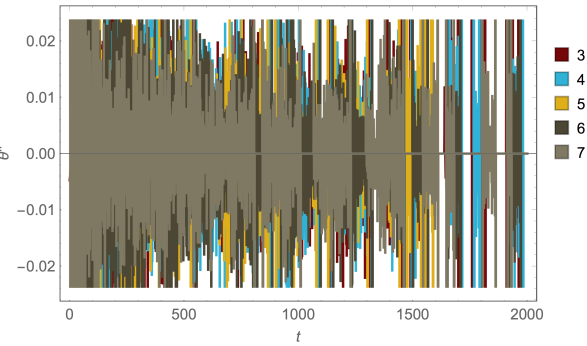


Figure 55 $\ddot{\theta}$ v.s. t of five trials

The results above clearly show the patterns achieved in the numerical simulation.

3.3.2 Error Analysis

An error analysis is done to verify the theoretical part. Starting from mathematically deducing the uncertainty, the x and y coordinates can be separately extracted and treated as two independent variables.

$$\begin{aligned} \phi &= \arcsin \frac{r}{R\theta} \\ &= \arcsin \frac{\sqrt{x^2 + y^2}}{R \arctan \frac{x}{y}} \end{aligned} \quad (3.13)$$

The uncertainty of x and y can be determined by formulae:

$$\begin{cases} \Delta_x = \sqrt{\frac{\sum_{i=1}^5 (x_i - \bar{x})^2}{5}} \\ \Delta_y = \sqrt{\frac{\sum_{i=1}^5 (y_i - \bar{y})^2}{5}} \end{cases} \quad (3.14)$$

Where $\bar{x} = x$, $\bar{y} = y$. We can get the expression of the uncertainty by taking the derivatives of the interpolation of ϕ as follows:

$$\begin{aligned} \Delta_\phi &= \sqrt{\left(\frac{\partial\phi}{\partial x}\right)^2 + \left(\frac{\partial\phi}{\partial y}\right)^2} \quad (3.15) \\ &= \Delta_x \left(\frac{y + 2x \arctan\left(\frac{y}{x}\right)}{\sqrt{1 - \frac{(x^2+y^2)^2}{\arctan^2\left(\frac{y}{x}\right)}} \arctan^2\left(\frac{y}{x}\right)} \right)^2 + \Delta_y \left(\frac{-x + 2y \arctan\left(\frac{y}{x}\right)}{\sqrt{1 - \frac{(x^2+y^2)^2}{\arctan^2\left(\frac{y}{x}\right)}} \arctan^2\left(\frac{y}{x}\right)} \right)^2 \\ &= \sqrt{\frac{\Delta_y x^2 + \Delta_x y^2 + 4(\Delta_x - \Delta_y)xy \arctan\left(\frac{y}{x}\right) + 4(\Delta_x x^2 + \Delta_y y^2) \arctan^2\left(\frac{y}{x}\right)}{\arctan^2\left(\frac{y}{x}\right)(-(x^2 + y^2)^2 + \arctan^2\left(\frac{y}{x}\right))}} \end{aligned} \quad (3.16)$$

According to the relationship above, the error can be calculated and plotted in Fig.56.

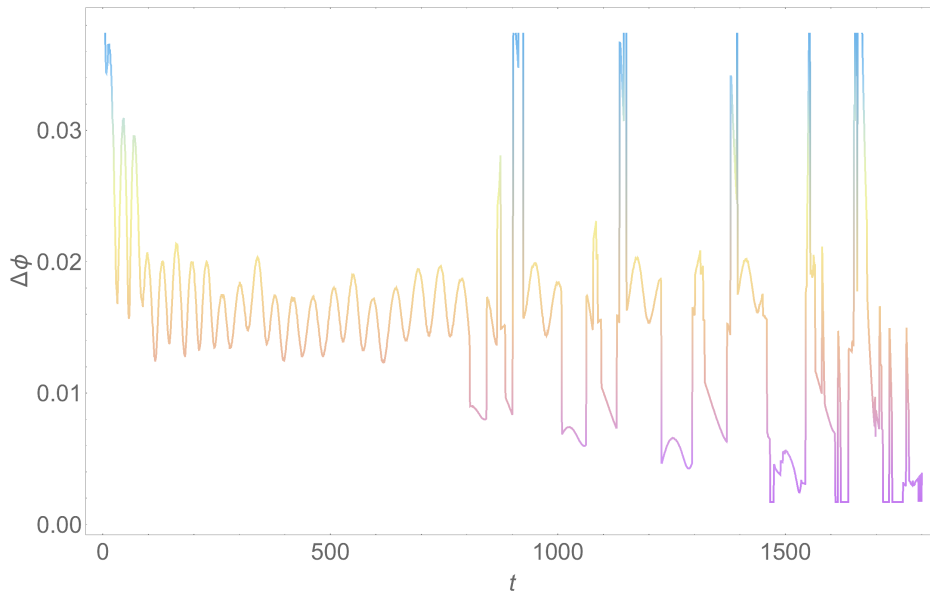


Figure 56 Calculated Error

The modified function in the range of the error function is plotted for comparison with

the calculated function, as shown in Fig.57.

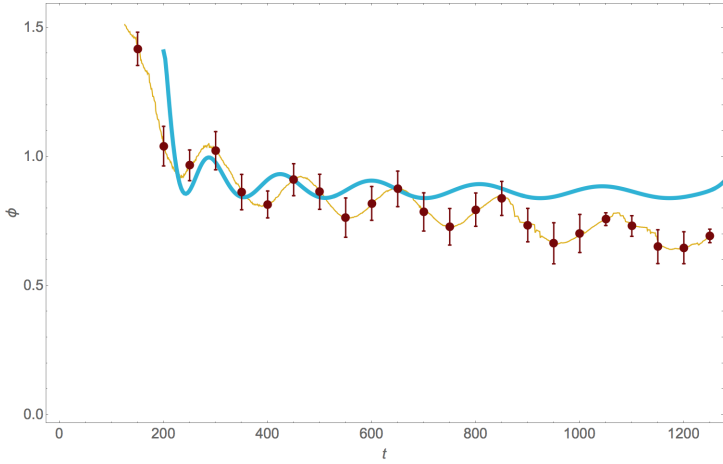


Figure 57 Comparison of the modified ϕ and the simulated ϕ

It is clear that the contour of the plot and oscillating frequencies of the theoretical and experimental motion are the same at the beginning. Then the experimental value falls in a relatively steep speed, which should be attributed to the air resistance and friction which are causing energy losses of the system. Thus, the ϕ angle will gradually tend to zero. Clearly, the theoretical is appropriate to explain this oscillating phenomenon and the energy loss effect can be studied more in future researches.

4 Conclusions

Through the theoretical part, we set up a valid physical model to address the physical phenomenon in the **Danza de los Voladores** which has not been previously studied. The characteristic oscillatory motion of the coordinates and the horizontal asymptote are studied by using appropriate approximations. Then, experiments are carried out which successfully verify the theoretical model, during when some minor problems are addressed by theory and the errors are within reasonable and acceptable range. Throughout the research, numerical simulations are also employed to prove the theories. Based on the results of the research, two major conclusions could be made:

- (1) The motion have non-conservative angular momentum, with a monotonic increasing angular velocity, but oscillatory angular acceleration.
- (2) The latitude angle ϕ is oscillatory and asymptotic during the motion, with a limit depending on the initial conditions.

5 Prospect

No study related to this phenomenon is done to the best of our knowledge and the research method used in this paper are based on the knowledge of our general physics honor course, analytical mechanics and interest in physics. Scientific computing software such as Mathematica and MATLAB are employed throughout the research. Beside the theory is established, analyzed and verified, experimental errors inevitably occurs during the study, such as the process of extracting the velocities of the bob. Also, the chaotic motion[12] is not taken into account using the current model. Thus, the research can be improved soon in the future with the knowledge of more advanced mechanics courses, more skills in computation and better equipment to conduct the experiments.

This phenomenon, coincidentally discovered, is explainable based on the model in this paper but not completely understood yet due to the complexity of the mathematical structure and quantities such as the Lagrangian. A better understanding of this phenomenon can help people understand more about the mathematical formulation of analytical mechanics and the correlation between math and physics. It can also help addressing more philosophical problems such as “If a physics problem is valid mathematically, is it ‘physical’?”, “Can every ‘math problems’ be made physical by some means?” and “What is the meaning of being ‘physical’?” Thus, it is worth future research with more powerful analyzing tools and knowledge on physics.

Reference

- [1] Danza de los voladores. https://en.wikipedia.org/wiki/Danza_de_los_Voladores.
- [2] Danza de los voladores. https://www.youtube.com/results?search_query=danza+delos+voladores+.
- [3] LD Akulenko and SV Nesterov. The stability of the equilibrium of a pendulum of variable length. *Journal of applied mathematics and mechanics*, 73(6):642–647, 2009.
- [4] Variable length pendulum. <https://physics.stackexchange.com/questions/327698/equation-of-motion-for-pendulum-with-variable-length?rq=1>.
- [5] A conical pendulum. <https://physics.stackexchange.com/questions/166026/a-conical-pendulum-a-textbook-claims-one-can-start-the-circular-motion-in-an-un>.
- [6] Involute. <https://en.wikipedia.org/wiki/Involute>.
- [7] Anton O Belyakov, Alexander P Seyranian, and Angelo Luongo. Dynamics of the pendulum with periodically varying length. *Physica D: Nonlinear Phenomena*, 238(16):1589–1597, 2009.
- [8] David Baraff. Linear-time dynamics using lagrange multipliers. In *Proceedings of the 23rd annual conference on Computer graphics and interactive techniques*, pages 137–146. ACM, 1996.
- [9] Mark Adler and Pierre Van Moerbeke. Linearization of hamiltonian systems, jacobi varieties and representation theory. *Advances in Mathematics*, 38(3):318–379, 1980.
- [10] Lev Davidovich Landau and EM Lifschic. *Course of theoretical physics. vol. 1: Mechanics*. Oxford, 1978.
- [11] Richard P Feynman, Robert B Leighton, and Matthew Sands. *The Feynman lectures on physics, Vol. I: The new millennium edition: mainly mechanics, radiation, and heat*, volume 1. Basic books, 2011.
- [12] Massimo Furi, Mario Martelli, Mike O’Neill, and Carolyn Staples. Chaotic orbits of a pendulum with variable length. *Electronic Journal of Differential Equations (EJDE)[electronic only]*, 2004:Paper–No, 2004.

Acknowledgements

The completion of this undertaking could not be possible without the assistance of so many people whose name may not be enumerated. Their contributions are gratefully acknowledged and sincerely appreciated. However, the group would like to express their special thanks to Shiqiang Deng, the best high school physics instructor in the world; Yongyuan Jiang, who offered us guidance and suggestions for the research; Guillermo Aboumrad, who offered inspiration to this question; Robin Hughes, who proposed the initial problem; and other physics teachers.



Coyolxauhqui [kojotʃa:mkɪ]
(Artistic Rendering of the Trajectory)

Appendix

List of Graphics

1	Danza de los Voladores (Dance of the Flyers)[2]	2
2	Details of the pole	2
3	The winding pendulum model	4
4	The two degrees of freedoms in the model	7
5	ϕ v.s. t plot of the result	8
6	θ v.s. t plot of the result	8
7	log-log plot of the result	9
8	Free body diagram of the conical pendulum	12
9	Linear fitting of the log-log plot	13
10	p v.s. t plot of the simulation	14
11	Free body diagram of the model	16
12	The two degrees of freedoms in the model	16
13	θ v.s. t plot.	17
14	ϕ v.s. t plot with different values of θ_0	18
15	ϕ v.s. t plot with different values of ϕ_0	18
16	ϕ v.s. t plot with different values of ϕ_0	19
17	ϕ v.s. t plot with different values of θ_0	19
18	Trajectory top view, $t = 0 \dots 2$	20
19	Trajectory top view, $t = 0 \dots 50$	20
20	Top view of trajectory with $t = 0 \dots 200$	20
21	Trajectory with comparison involute of a circle in different instances	21
22	Trajectory side view, $t=0 \dots 2$	21
23	Trajectory side view, $t=0 \dots 200$	21
24	3D parametric plot with $t = 0 \dots 10$	21
25	3D parametric plot with $t = 0 \dots 200$	21
26	Bottom view of the platform	24
27	Materials used in the experiment	25
28	Experimental setup	26
29	Trajectory of the bob in Trial 1	27
30	Trajectory of the bob in Trial 2	27
31	ϕ v.s. t plot of trial 1	28
32	ϕ v.s. t plot of trial 2	28
33	Linear fit of the log-log plot 1	28
34	Linear fit of the log-log plot 2	29
35	The light used to trace the position of the bob	29
36	The way to determine R	29
37	Trial 3 Overview	30
38	Trial 3 Sideview	30
39	Trial 3 θ with noise	31

40	Trial 3 α with noise	31
41	Trial 3 θ with noise reduced	31
42	Trial 3 α with noise reduced	31
43	The overview data of motion of five trials 3-7	32
44	The side-view data of motion of trials 3-7	32
45	Photographs of the sudden-sliding phenomenon	33
46	Zoomed diagram of the thread	34
47	Relationship between rhp , a and b	35
48	The changing of θ over time	36
49	The definition of α , \mathbf{r}	37
50	The changing of α over time	37
51	The changing of ϕ over time	38
52	$\dot{\phi}$ v.s. t of five trials	39
53	$\ddot{\phi}$ v.s. t of five trials	39
54	$\dot{\theta}$ v.s. t of five trials	39
55	$\ddot{\theta}$ v.s. t of five trials	39
56	Calculated Error	40
57	Comparison of the modified ϕ and the simulated ϕ	41

List of Tables

List of Tables

1	List of Variables	5
2	Initial conditions of the simulation	8
3	Initial conditions with different values of θ_0	18
4	Initial conditions with different values of ϕ_0	18
5	Initial conditions with different values of $\dot{\phi}_0$	19
6	Initial conditions with different values of θ_0	19
7	The conditions of the experiment	30

Mathematica Codes

```
(*CommonArea*)
Clear["`*"];
tp = 20000;
cond = {td → θ'[t], t → θ[t], p → φ[t], pd → φ'[t], m → 1, R → 1, g → 1};
xcond = {td → θ'[t], t → θ[t], p → φ[t], pd → φ'[t]};
rcond = {θ'[t] → tdd, θ[t] → td, θ[t] → t, φ[t] → p, φ'[t] → pd, φ'[t] → pdd};

(*Spherical Pendulum Version*)
L =  $\frac{1}{2} m pd^2 l^2 + g m l \text{Cos}[p] + \frac{1}{2} m l^2 td^2 \text{Sin}[p]^2$ ;
H =  $\frac{1}{2} m pd^2 l^2 - g m l \text{Cos}[p] + \frac{1}{2} m l^2 td^2 \text{Sin}[p]^2$ ;

(*Simplified Version*)
L =  $\frac{1}{2} m pd^2 R^2 t^2 + \frac{1}{2} m R^2 td^2 + g m R t \text{Cos}[p] + \frac{1}{2} m R^2 t^2 td^2 \text{Sin}[p]^2$ ;
EE =  $\frac{1}{2} m pd^2 R^2 t^2 + \frac{1}{2} m R^2 td^2 - g m R t \text{Cos}[p] + \frac{1}{2} m R^2 t^2 td^2 \text{Sin}[p]^2$ ;

(*Revolute Version*) L =  $\frac{1}{2} m (pd R t - R td \text{Sin}[p])^2 +$ 
 $\frac{1}{2} m (R td - R td \text{Cos}[p])^2 + g m R t \text{Cos}[p] + \frac{1}{2} m R^2 t^2 td^2 \text{Sin}[p]^2$ ;
H =  $\frac{1}{2} m (pd R t - R td \text{Sin}[p])^2 + \frac{1}{2} m (R td - R td \text{Cos}[p])^2 -$ 
 $g m R t \text{Cos}[p] + \frac{1}{2} m R^2 t^2 td^2 \text{Sin}[p]^2$ ;
P =  $m R^2 t^2 \text{Sin}[p]^2 td$ ;

Eva = Evaluate@{D[L, t], D[L, td], D[L, p], D[L, pd]};
Equ = Eva /. cond;
Equ1 = Equ[[1]] == D[Equ[[2]], t];
Equ2 = Equ[[3]] == D[Equ[[4]], t];
s1 = NDSolve[{Equ1, Equ2, θ'[0] == 0,
    φ'[0] == 10, θ[0] == 0.001, φ[0] == 0.001}, {θ, φ}, {t, 0, tp}];
s2 = NDSolve[{Equ1, Equ2, θ'[0] == 0, φ'[0] == 10, θ[0] == 0.001, φ[0] == Pi/4},
    {θ, φ}, {t, 0, tp}];
s3 = NDSolve[{Equ1, Equ2, θ'[0] == 0, φ'[0] == 10, θ[0] == 0.001, φ[0] == Pi/3},
    {θ, φ}, {t, 0, tp}];
s4 = NDSolve[{Equ1, Equ2, θ'[0] == 0, φ'[0] == 10, θ[0] == 0.001,
    φ[0] == Pi/2 + 0.4454711}, {θ, φ}, {t, 0, tp}]; (*Strange point +- inverse*)
s5 = NDSolve[{Equ1, Equ2, θ'[0] == 0, φ'[0] == 10, θ[0] == 0.001, φ[0] == 2 Pi/3},
    {θ, φ}, {t, 0, tp}];
s6 = NDSolve[{Equ1, Equ2, θ'[0] == 0, φ'[0] == 10, θ[0] == 0.001,
    φ[0] == Pi - 0.0632244444}, {θ, φ}, {t, 0, tp}]; (*Strange Point 2*)
```

```

(*Fancy Solver Input*)
tp = 100;
k = 6;
Grid@Map[InputField[#, FieldSize -> 6, FieldHint -> "#"] &,
  Dynamic /@Table[#[i], {i, 1, k}] & /@{p, tt, pd, td}, {2}]
Dynamic /@Table[#[i], {i, 1, k}] & /@{p, tt, pd, td} // TableForm
Eva = Evaluate@{D[L, t], D[L, td], D[L, p], D[L, pd]};
Equ = Eva /. cond;
Equ1 = Equ[[1]] == D[Equ[[2]], t];
Equ2 = Equ[[3]] == D[Equ[[4]], t];

(*Fancy Solver Main*)
{s0, s1, s3, s4, s5, s6} = Flatten[
  MapThread[NDSolve[{Equ1, Equ2,  $\theta'[0] == \#4$ ,  $\phi'[0] == \#3$ ,  $\theta[0] == \#2$ ,  $\phi[0] == \#$ },
    { $\theta, \phi$ }, {t, 0, tp}] &, Table[#[i], {i, 1, k}] & /@{p, tt, pd, td}], 1];

(*Ploter*)
{{Plot[Evaluate@Flatten@(ReplaceAll[#[ $\phi[t]$ ] &@{s1, s2, s3, s4, s5, s6}),
  {t, 0, tp}, PlotRange -> {{0, tp}, Automatic}, AspectRatio -> 0.5,
  PlotLabel -> "纬度 latitude", PlotLegends -> {1, 2, 3, 4, 5, 6},
  ImageSize -> Large, PlotStyle -> {, , , , , \phi'[t]] &@{s1, s2, s3, s4, s5, s6}),
  {t, 0, tp}, PlotRange -> {{0, tp}, Automatic}, AspectRatio -> 0.5,
  PlotLabel -> "纬度速度 vp", PlotLegends -> {1, 2, 3, 4, 5, 6}, ImageSize -> Large],
  Plot[Evaluate@Flatten@(ReplaceAll[#[ $\theta'[t] \sin[\phi[t]]^2$ ] &@
    {s1, s2, s3, s4, s5, s6}), {t, 0, tp},
  PlotRange -> {{0, tp}, Automatic}, AspectRatio -> 0.5, PlotLabel -> "纬度速度 vp",
  PlotLegends -> {1, 2, 3, 4, 5, 6}, ImageSize -> Large]}],
{LogLogPlot[Evaluate@Flatten@(ReplaceAll[#[ $\theta[t]$ ] &@{s1}),
  {t, 0, tp}, PlotRange -> {{0, tp}, Automatic},
  AspectRatio -> 0.5, PlotLabel -> "经度 longitude",
  PlotLegends -> {1, 2, 3, 4, 5, 6}, ImageSize -> Large, Frame -> True],
  Plot[Evaluate@Flatten@(ReplaceAll[#[ $\theta'[t]$ ] &@{s1, s2, s3, s4, s5, s6}),
  {t, 0, tp}, PlotRange -> {{0, tp}, Automatic}, AspectRatio -> 0.5,
  PlotLabel -> "经度速度 vt", PlotLegends -> {1, 2, 3, 4, 5, 6}, ImageSize -> Large]},
{Plot[Evaluate@Flatten@(ReplaceAll[#[H /. cond] &@{s1, s2, s3, s4, s5, s6}),
  {t, 0, tp}, PlotRange -> {{0, tp}, Automatic}, AspectRatio -> 0.5,
  PlotLabel -> "哈密顿量 H", PlotLegends -> {1, 2, 3, 4, 5, 6}, ImageSize -> Large],
  Plot[Evaluate@Flatten@(ReplaceAll[#[EE /. cond] &@{s1, s2, s3, s4, s5, s6}),
  {t, 0, tp}, PlotRange -> {{0, tp}, Automatic}, AspectRatio -> 0.5,
  PlotLabel -> "能量 E", PlotLegends -> {1, 2, 3, 4, 5, 6}, ImageSize -> Large],
  Plot[Evaluate@Flatten@(ReplaceAll[#[P /. cond] &@{s1, s2, s3, s4, s5, s6}),
  {t, 0, tp}, PlotRange -> {{0, tp}, Automatic}, AspectRatio -> 0.5, PlotLabel ->
  "角动量 P", PlotLegends -> {1, 2, 3, 4, 5, 6}, ImageSize -> Large]}] // TableForm

```

```

(*LinearFit*)LinearModelFit[
  Table[Flatten@{Log[t], Log[( $\theta[t]$  /. s1)]} /. t  $\rightarrow$  a, {a, 1, tp, tp/10000}], x, x]
Show[ListPlot[Table[Flatten[{Log[t], Log[( $\theta[t]$  /. s1)]} /. t  $\rightarrow$  a,
  {a, 1, tp,  $\frac{tp}{10000}$ }], PlotStyle  $\rightarrow$  Red], Plot[%425[x], {x, 0, Log[200]}]]

(*OtherStuff*)
CoolColor[z_] := RGBColor[z, 1 - z, 1];
CoolColor /@ Range[0, 1, 1/5]

(*Redefinition*)
x = R Cos[ $\theta[t]$ ] +  $\theta[t]$  R Sin[ $\phi[t]$ ] Sin[ $\theta[t]$ ];
y = R Sin[ $\theta[t]$ ] -  $\theta[t]$  R Sin[ $\phi[t]$ ] Cos[ $\theta[t]$ ];
z = - $\theta[t]$  R Cos[ $\phi[t]$ ];
x1 = R Cos[ $\theta[t]$ ] +  $\theta[t]$  R Sin[ $\theta[t]$ ];
y1 = R Sin[ $\theta[t]$ ] -  $\theta[t]$  R Cos[ $\theta[t]$ ];

(*2D Trajectory Plot*)Show[
  ParametricPlot[Evaluate@Flatten[{x, y}, {x1, y1}] /. {R  $\rightarrow$  (R /. cond)} /. s1, 1],
  {t, 0, tp}, PlotStyle  $\rightarrow$  {Blue, Directive[Red, Dashed]},
  PlotLegends  $\rightarrow$  {"Trajectory", "Comparision"},
  Graphics[{Blue, Disk[{0, 0}, R /. cond]}]]

(*3D Trajectory Plot*)
Rasterize[ParametricPlot3D[{x, y, z} /. {R  $\rightarrow$  (R /. cond)} /. s1, {t, 0, tp},
  ColorFunction  $\rightarrow$  CoolColor] /. Line[pts_, rest___] :> Tube[pts, 0.05, rest],
  ImageSize  $\rightarrow$  1000, RasterSize  $\rightarrow$  2000]

(*Movable Trajectory Plot*)Manipulate[
  ParametricPlot[Evaluate@Flatten[{x, y}, {x1, y1}] /. {R  $\rightarrow$  (R /. cond)} /. s1, 1],
  {t, tx - 10, tx}, PlotStyle  $\rightarrow$  {Blue, Red},
  PlotRange  $\rightarrow$  {{-300, 300}, {-300, 300}}, {tx, 10, tp}]

(*Importing Experiment Files*)
data = Import[FileNameJoin[{Downloads, "IMG_3533", #}]] & /@
  Import[FileNameJoin[{Downloads, "IMG_3533"}]][[2 ;; ;; 10]];

(*Binarizing & Image Processing*)
datab = Binarize[#, 0.6] & /@ data;
ImageAdd@@ datab

(*Processing*)DynamicModule[{pt = {0, 0}}, {LocatorPane[
  Dynamic[pt], #, Appearance  $\rightarrow$  Style["o", Red]], Dynamic[pt]}] & /@ data
StringTake[ToString@#, {20, 32}] &

```

```

(*Plotting*)
ListLinePlot[Subtract[#, data[[1]]] & /@ data, AspectRatio → 1,
  PlotRange → {{-500, 360}, {-600, 260}}, ColorFunction →
  Function[{x, y}, ColorData["ValentineTones"][1 - Sqrt[y^2 + x^2] / 650]],
  PlotStyle → Thickness[0.01], Frame → True, ColorFunctionScaling → False]
Rasterize[#, ImageSize → 1000, RasterSize → 2000] & /@
{ListLinePlot[p, Mesh → Full, MeshStyle → Directive[PointSize[Medium],
  ColorData["AvocadoColors"][0.25]], AxesLabel → {"t", "θ"},
  PlotStyle → ColorData["AvocadoColors"][0.7]], ListLinePlot[
  ArcTan[#[[2]] / #[[1]]] & /@ (Subtract[#, data[[1]]] & /@ Drop[data, 1]),
  Mesh → Full, PlotStyle → ColorData["AvocadoColors"][0.8],
  MeshStyle → Directive[ColorData["AvocadoColors"][0.4]], AspectRatio → 1 / 9]}

(*MATLAB data Processing*)GraphicsRow[
  Table[ListPlot[data5B[[1 ;; d]], PlotRange → {{0, Max[First@Transpose@data5B]},
    {0, Max[Last@Transpose@data5B]}}, Frame → True, FrameTicks → None],
    {d, 0, Quotient[Count[data5B, _], 300] 300, 300}], -9]

(*Importing*)
Clear[data, data0, k];
Table[data[i] = (First@Import@FindFile["Trial" <> ToString[i] <> "B.mat"]) ~
  Dot~{{1, 0}, {0, -1}}, {i, 1, 5}];
Table[data0[i] = Subtract[#, (data[i][[60]] + data[i][[90]]) / 2] & /@
  Drop[data[i], 60], {i, 1, 5}];
k = {{10, -20}, {10, -50}, {20, -60}, {10, 10}, {1, -20}};
Table[data0[i] = Subtract[#, k[[i]]] & /@ data0[i], {i, 1, 5}];
data0[2] = Drop[data0[2], 170];
{Table[ListPlot[data0[i]], {i, 1, 5}] // TableForm

```

```

(*Processing  $\theta$ *)
Clear[t];
Table[Module[{a, s, i, j}, Quiet[For[p = {};
  i = 0;
  a = 0;
  j = 1, j <= Count[#, _], j++,
  s = Module[
    {h := (i Pi + (ArcTan[#[[2]]/#[[1]]) /. {Indeterminate -> a - i Pi})},
    If[h < a, i++, Indeterminate];
    If[h - a < 3, h, i = i - 1; a]
  ] &@#[[j]]; a = s; p = Append[p, a]]] &@data0[i];
  t[i] = p, {i, 1, 5}];
Clear[r, rs];
Table[r[i] = Sqrt[(#[[2]]^2 + #[[1]]^2)] &/@data0[i], {i, 1, 5}];

Table[Module[{a, b, c, h}, For[i = 1;
  a = #[[1]];
  s = {}, i <= Count[#, _], i++, b = #[[i]];
  h = If[Abs[b - a] > 80, a, b];
  s = Append[s, h];
  a = h] &@r[k];
  rs[k] = s, {k, 1, 5}];

(*Processing  $\alpha$ *)Quiet[Table[
  t[i] = ArcTan[#[[2]]/#[[1]]] &/@data0[i] /. Indeterminate -> 0, {i, 1, 5}];
Table[Module[{a, b, c, h}, For[i = 1;
  a = #[[1]];
  s = {}, i <= Count[#, _], i++, b = #[[i]];
  h = If[Abs[b - a] > 0.3, a, b];
  s = Append[s, h];
  a = h] &@t[k];
  ts[k] = s, {k, 1, 5}];
Clear[r, rs];
Table[r[i] = Sqrt[(#[[2]]^2 + #[[1]]^2)] &/@data0[i], {i, 1, 5}];

Table[Module[{a, b, c, h}, For[i = 1;
  a = #[[1]];
  s = {}, i <= Count[#, _], i++, b = #[[i]];
  h = If[Abs[b - a] > 20, a, b];
  s = Append[s, h];
  a = h] &@r[k];
  rs[k] = s, {k, 1, 5}];

```

```

(*Plotting*)
Transpose@Table[{ListLinePlot[t[i], Mesh → All, MeshStyle →
  Directive[PointSize[Small], Darker@Darker@Brown], Filling → Axis,
  ColorFunction → "WatermelonColors", Frame → True, FrameLabel → {"t",  $\theta$ }],
  ListLinePlot[rs[i]/20, Mesh → All, MeshStyle →
  Directive[PointSize[Small], Darker@Darker@Brown],
  Filling → Axis, ColorFunction → "WatermelonColors", Frame → True,
  FrameLabel → {"t",  $l \sin[\phi]$ }], {i, 1, 5}] // TableForm
ListLinePlot[Table[Abs@ArcSin[Quiet[(rs[i]/t[i]/20)] /. Indeterminate → 0],
  {i, 1, 5}], PlotLegends → {"1", "2", "3", "4", "5"}, Mesh → None,
  PlotStyle → {■, ■, ■, ■, ■}, Frame → True, FrameLabel → {t,  $\phi$ }]
ListLinePlot[Table[ts[i], {i, 1, 5}], PlotStyle → {■, ■, ■, ■, ■},
  Frame → True, FrameLabel → {t,  $\alpha$ }, PlotLegends → {"1", "2", "3", "4", "5"}]
Z = Plus@@Table[Abs@ArcSin@Take[rs[i]/t[i]/20, 1800], {i, 1, 5}]/5;
ListPlot[{Z, Z + F, Z - F}, PlotLegends → {"1", "2", "3", "4", "5"},
  Mesh → None, PlotStyle → {■, ■, ■}, Frame → True, FrameLabel → {t,  $\phi$ }]

(*Error Analysis*)
Bar = Plus@@Table[Take[data0[j], 1800], {j, 1, 5}];
ab =
  Transpose[Sqrt[Plus@@Table[(Take[data0[i], 1800] - Bar/5)^2, {i, 1, 5}]/5]];
T = Plus@@Table[Take[t[j], 1800], {j, 1, 5}]/5;
abBar = Flatten[{ab, Transpose@Bar, {T}}, 1];
F =
  MapThread[Abs[Simplify@Sqrt[a D[ArcSin[(x^2 + y^2)/ArcTan[(y/x)]/20], x]^2 +
    b D[ArcSin[(x^2 + y^2)/ArcTan[(y/x)]/20], y]^2] /.
    {ArcTan[ $\frac{y}{x}$ ] → #5, a → #1, b → #2, x → #3, y → #4, Abs' → Abs}] &, abBar];

```

```

(*Graphix Plotting*)CoolColor /@Range[0, 1, 1/10] Show[
  Graphics3D[{FaceForm[Red], Cylinder[{0, 0, -0.3}, {0, 0, 2.5}]}], Boxed → False],
  ParametricPlot3D[{Sin[u], Cos[u], u/300}, {u, 0, 500}, PlotStyle → Cyan,
    PlotRange → All, Boxed → False] /. Line[pts_, rest___] :=> Tube[pts, 0.01, rest],
  ParametricPlot3D[{1, u, -u}, {u, 0, 2}, PlotStyle → Cyan, PlotRange → All,
    Boxed → False] /. Line[pts_, rest___] :=> Tube[pts, 0.01, rest],
  Graphics3D[{
    FaceForm[Red],
    Ball[{1, 2, -2}, 0.3],
    FaceForm[Red], Arrow[Tube[{1, 2, -2}, {1, 2, -4}]]],
    FaceForm[Red], Arrow[Tube[{1, 2, -2}, {1, 1, -1}]]],
    Arrowheads[{-0.03, 0.03}],
    FaceForm[Cyan], Arrow[Tube[{0, 0, -0.3}, {0, 1, -0.3}]]],
    Text[Style["R", Bold, 30, Cyan], {0, 0.5, -0.8}],
    Text[Style["m", Bold, 30, Cyan], {1, 2, -2}],
    Text[Style[OverVector["T"], Bold, 30, Cyan], {1, 1.5, -1}],
    Text[Style["m" OverVector["g"], Bold, 30, Cyan], {1, 2, -4.3}],
    Text[Style["l", Bold, 30, Cyan], {1, 2/5*2, -2/5*2}]
  ], Boxed → False]]

Show[
  Graphics3D[{FaceForm[Red], Cylinder[{0, 0, -0.3}, {0, 0, 2.5}]}], Boxed → False],
  ParametricPlot3D[{Sin[u], Cos[u], u/300}, {u, 0, 500}, PlotStyle → Cyan,
    PlotRange → All, Boxed → False] /. Line[pts_, rest___] :=> Tube[pts, 0.01, rest],
  ParametricPlot3D[{1, u, -u}, {u, 0, 2}, PlotStyle → Cyan, PlotRange → All,
    Boxed → False] /. Line[pts_, rest___] :=> Tube[pts, 0.01, rest],
  Graphics3D[{
    FaceForm[Red],
    Ball[{1, 2, -2}, 0.3],
    FaceForm[Red], Arrow[Tube[{1, 0, 0}, {1, 0, -2}]]],
    FaceForm[Red], Arrow[Tube[{0, 0, -0.3}, {-1.2, -0.8, -0.3}]]],
    FaceForm[Cyan], Tube[{0, 0, -0.3}, {1, 0, -0.3}],
    Text[Style["θ", Bold, 30, Cyan], {0, 0.2, -0.4}],
    Text[Style["φ", Bold, 30, Cyan], {1, 0.5, -0.8}]
  ], Boxed → False],
  (ParametricPlot3D[{0.5 Sin[u], 0.5 Cos[u], -0.3}, {u, -2.15, 1.55},
    PlotStyle → Cyan, PlotRange → All, Boxed → False] /. Line[pts_, rest___] =>
    {Arrowheads → Small, Arrow[#]} &@Tube[pts, 0.01, rest]),
  (ParametricPlot3D[{1, 0.5 Cos[u], 0.5 Sin[u]}, {u, -Pi/2, -Pi/4},
    PlotStyle → Cyan, PlotRange → All, Boxed → False] /. Line[pts_, rest___] =>
    {Arrowheads → Small, Arrow[#]} &@Tube[pts, 0.01, rest])]

```

```
Show[Graphics3D[{{FaceForm[Red], Cylinder[{{0, 0, -0.3}, {0, 0, 2.5}}],
  FaceForm[Red], Cylinder[{{0, 0, -4}, {0, 0, 7}], 0.3}}, Boxed → False],
ParametricPlot3D[{Sin[u], Cos[u], u/300}, {u, 0, 500}, PlotStyle → Cyan,
  PlotRange → All, Boxed → False] /. Line[pts_, rest___] := Tube[pts, 0.01, rest],
ParametricPlot3D[{1, u, -u}, {u, 0, 2}, PlotStyle → Cyan, PlotRange → All,
  Boxed → False] /. Line[pts_, rest___] := Tube[pts, 0.01, rest],
Graphics3D[{
  FaceForm[Red],
  Ball[{1, 2, -2}, 0.3],
}], Boxed → False]]

Show[
Graphics3D[{{FaceForm[Red], Cylinder[{{0, 0, -1}, {0, 0, 2.5}}], Boxed → False}},
ParametricPlot3D[{Sin[u], Cos[u], u/300}, {u, 0, 500}, PlotStyle → Cyan,
  PlotRange → All, Boxed → False] /. Line[pts_, rest___] := Tube[pts, 0.01, rest],
ParametricPlot3D[{
  {Sqrt[3], u, -u},
  {-Sqrt[3], -u, -u},
  {u, -Sqrt[3], -u},
  {-u, Sqrt[3], -u}
}, {u, 0, 2}, PlotStyle → Cyan, PlotRange → All, Boxed → False] /.
  Line[pts_, rest___] := Tube[pts, 0.01, rest],
ParametricPlot3D[{
  {0, u, 0},
  {0, -u, 0},
  {u, 0, 0},
  {-u, 0, 0}
}, {u, 0, Sqrt[3]}, PlotStyle → Cyan, PlotRange → All, Boxed → False] /.
  Line[pts_, rest___] := Tube[pts, 0.01, rest],
Graphics3D[{
  FaceForm[Red],
  Ball[{Sqrt[3], 2, -2}, 0.3],
  Ball[{-Sqrt[3], -2, -2}, 0.3],
  Ball[{2, -Sqrt[3], -2}, 0.3],
  Ball[{-2, Sqrt[3], -2}, 0.3],
  FaceForm[Cyan], Arrow[Tube[{{0, 0, -1}, {-1.5, -0.8, -1}}]],
  FaceForm[Cyan], Arrow[Tube[{{0, 0, -1}, {0.8, 0.6, -1}}]],
  Text[Style["R", Bold, 30, Cyan], {0.8, 0.6, -1}/3],
  Text[Style["r", Bold, 30, Cyan], {-1.5, -0.8, -1}/2]
}], Boxed → False],
RegionPlot3D[2 < x^2 + y^2 < 3, {x, -2, 2}, {y, -2, 2}, {z, -1 + 0.4, 0},
  PlotStyle → Red, Mesh → None, BoundaryStyle → None, Boxed → False],
Boxed → False, BoundaryStyle → None]
```

```
Show[Graphics[{{Red, Disk[{0, 0}, {2, 3}]}},
ParametricPlot[{2 Sin[u], 3 Cos[u]},
{u, 3 Pi/2, 3 Pi}, PlotStyle -> Directive[Thickness[0.07], Red]],
ParametricPlot[{2 Sin[u], 3 Cos[u]}, {u, 3 Pi/2, 3 Pi/2 + 0.3},
PlotStyle -> Directive[Thickness[0.07], Red]], ParametricPlot[
{-2, -u}, {u, 0, Pi}, PlotStyle -> Directive[Thickness[0.07], Red]],
ParametricPlot[{-2, -u}, {u, 0, Pi - 2.7},
PlotStyle -> Directive[Thickness[0.07], Red]],
ParametricPlot[{3^2/2 * Sin[u] + 3^2/2 - 2, 3^2/2 Cos[u]},
{u, 0, 2 Pi}, PlotStyle -> Directive[Thickness[0.02], Red]],
Graphics[{{Red, Arrowheads[{-0.1, 0.1}], Arrow[{{-2, 0}, {3^2/2 - 2, 0}]},
Text[Style[" $\rho = \frac{b^2}{a}$ ", Bold, 30, Red], {0, 1}]}]
] Show[Graphics3D[{{FaceForm[Red], Cylinder[{{0, 0, -1.3}, {0, 0, 2.5}]},
FaceForm[Red], Arrow[Tube[{{1, -0.35, 0.4}, {1, -0.35, -0.2}]}]},
FaceForm[Red], Arrow[Tube[{{1, -0.35, 0.4}, {1, -0.35, 1.4}]}]},
FaceForm[Red], Arrow[Tube[{{1, -0.35, 0.4}, {2, -0.7, 0.4}]}]},
Text[Style["m" OverVector["g"], Bold, 30, Red], {1, -0.35, -0.2}],
Text[Style[OverVector["f"], Bold, 30, Red], {1, -0.35, 1.4}],
Text[Style[OverVector["N"], Bold, 30, Red], {2, -0.7, 0.4}],
Text[Style[OverVector["T"], Bold, 30, Red], {1.1, 1.2 u, -u + 0.23} /. u -> 1.5],
Text[Style[OverVector["T"], Bold, 30, Red], {0.3, 1.2 u, -u + 0.23} /. u -> -1.9],
FaceForm[Red], Arrow[Tube[Evaluate[
{{1.1, 1.2 u, -u + 0.23} /. u -> -0.15, {1.1, 1.2 u, -u + 0.23} /. u -> 1.5}]]],
Arrow[Tube[Evaluate[{{0.99, 1.2 u, -u + 0.23} /. u -> -0.4,
{0.3, 1.2 u, -u + 0.23} /. u -> -1.9}]]]], Boxed -> False],
ParametricPlot3D[{Sin[u], Cos[u], Sin[u - Pi/1.3] + 1}, {u, 2, 2 Pi},
PlotStyle -> Red, PlotRange -> All, Boxed -> False] /.
Line[pts_, rest___] := Tube[pts, 0.1, rest],
ParametricPlot3D[{Sin[u], Cos[u], Sin[u - Pi/1.3] + 1},
{u, 1.7, 2}, PlotStyle -> Red, PlotRange -> All, Boxed -> False] /.
Line[pts_, rest___] := Tube[pts, 0.1, rest],
ParametricPlot3D[{1, 1.2 u, -u + 0.23}, {u, -0.1, 3},
PlotStyle -> Red, PlotRange -> All, Boxed -> False] /.
Line[pts_, rest___] := Tube[pts, 0.1, rest], BoundaryStyle -> None]
```

Matlab Code

Table of Contents

Importing image	1
Convert RGB to Grayscale	1
Finding max value	1
Converting	2
Saving	2

Importing image

```
Number='3'  
Letter='A'  
place=join(['/Trial',Number,'/Trial',Number,Letter]);  
[n,m]=size(dir(join(['/Users/VanLadmon/Downloads',place])));  
for i=1:n-3  
    l=5-length(num2str(i));  
    z=zeros(1,l);  
    t='_';  
    for k=1:l  
        t=join([t,num2str(z(k))]);  
    end  
    I{i}=imread(join(['/Users/VanLadmon/Downloads',place,'/  
Trial',Number,Letter,t,num2str(i),'.jpg']));  
end
```

```
Number =  
  
    '3'
```

```
Letter =  
  
    'A'
```

Convert RGB to Grayscale

```
for i=1:n-3  
J{i}=rgb2gray(I{i});  
end
```

Finding max value

```
for i=1:n-3  
[v,ind]=max(J{i});  
[v1,ind1]=max(max((J{i})));  
X{i}=[ind(ind1),ind1];  
if v1<50
```

```
X{i}=[0,0];  
end  
end
```

Converting

```
R=[];  
for i=1:n-3  
    for k=1:2  
        R(i,k)=X{i}(k);  
    end  
end
```

Saving

```
save('Trial3A.mat','R')
```

Published with MATLAB® R2017b

Brief Introduction of Team Members and Instructors

Team Members

1. Zhaoyi Li

Grade 12, Harbin Normal University High School.

2. Sifei Zhang

Grade 12, Dalian Yuming High School.

Instructors

1. Shiqiang Deng

Graduated from Tsinghua University. At present, he is a physics teacher of Harbin Normal University High School and he is the instructor of Chinese Physics Olympiad (CPhO).

2. Yongyuan Jiang

He is the professor of Department of Physics, Harbin Institute of Technology.